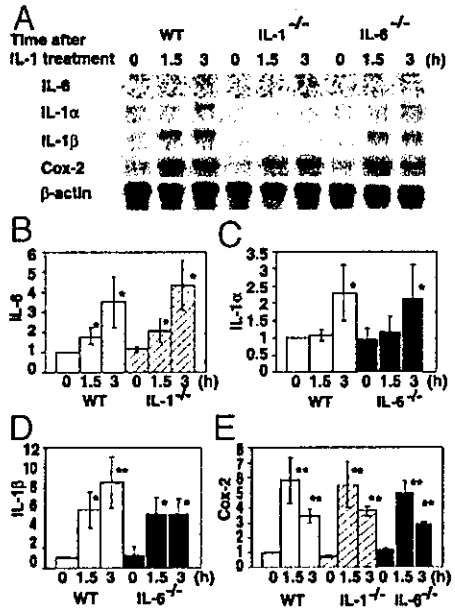

FIG. 2. Expression of the mRNA for *IL-6*, *IL-1α*, *IL-1β*, and *Cox-2* in the diencephalon after iv injection with IL-1α. A, Northern blot hybridization. B-E, relative radioactivity of the bands corresponding to *IL-1α*, *IL-1β*, IL-6, and *Cox-2* mRNA normalized against the intensity of the *β-actin* band. Data show the averages and the SD of three independent experiments. WT, Wild-type mice (*open bars*); IL-$1^{-/-}$, *IL-1α/β*-deficient mice (*stripe bars*); IL-$6^{-/-}$, *IL-6*-deficient mice (*filled bars*). *, $P < 0.05$; **, $P < 0.001$.

45 min, and 1 h 45 min to 8 h 45 min after IL-1α injection, compared with saline-injected *IL-1α/β*-deficient mice (#, $P < 0.05$). Interestingly, the febrile response of *IL-1α/β*-deficient mice was higher than that of wild-type mice (at 1 h 45 min to 2 h, 2 h 30 min, 4 h to 7 h 15 min, and 8 h to 8 h 15 min; *, $P < 0.05$). In contrast, IL-1-injected *IL-6*-deficient mice showed no elevation of body temperature at any time points relative to saline-injected *IL-6*-deficient mice (Fig. 1B). Similar results were obtained in another two experiments in which 10 μg/kg BW IL-1α was injected and body temperature was measured every 90 min. These results indicate that endogenous *IL-1* induction in the brain is not necessary for the development of fever, whereas *IL-6* is essential.

Induction of IL-6, IL-1α, IL-1β, and Cox-2 expression in the brain by IL-1α

We next examined the time course of mRNA expression for the *IL-6*, *IL-1α*, *IL-1β*, and *Cox-2* genes in the brain after IL-1α injection (Fig. 2). In wild-type mice, *Cox-2* and *IL-1β* were already strongly induced 1.5 h after injection of IL-1α, followed by *IL-6* and *IL-1α* induction after 3 h. Similarly, in *IL-1α/β*-deficient mice, *Cox-2* was strongly induced 1.5 h after the injection and *IL-6* induction followed 3 h after the injection, as observed in wild-type mice. In the case of *IL-6*-deficient mice, *Cox-2* and *IL-1β* were also induced 1.5 h after the injection and *IL-1α* was induced 3 h after the injection, as in wild-type mice. Similar results were obtained in two additional independent experiments using mRNAs from the whole brains. These results show that endogenous IL-1 and IL-6 are not necessary for the induction of *Cox-2* and that *IL-6* induction occurs later than that of *Cox-2*, suggesting that *IL-6* is induced downstream of PGE_2.

Suppression of IL-1-induced IL-6 expression by indomethacin

We next analyzed the effect of indomethacin, an inhibitor of cyclooxygenases, on the expression of *IL-6* to examine PGE_2 dependency of the *IL-6* expression. The expression of *IL-6* was measured at 0 h (basal level) and 3 h after IL-1 injection with or without indomethacin treatment. The administration of indomethacin 30 min before IL-1 injection strongly suppressed *IL-6* transcription (Fig. 3). By this treatment, the Cox-2 expression was not inhibited and was rather induced by the treatment itself, even in the absence of IL-1α treatment. Under these conditions, fever development was completely suppressed, in agreement with previous reports (data not shown; see Refs. 14, 18). These results suggest that *IL-6* expression is dependent on PGE_2 production.

Discussion

It is well known that intracerebroventricular administration of IL-1 induces fever development. Furthermore, we demonstrated previously that a febrile response triggered by an injection of turpentine was accompanied by a significant

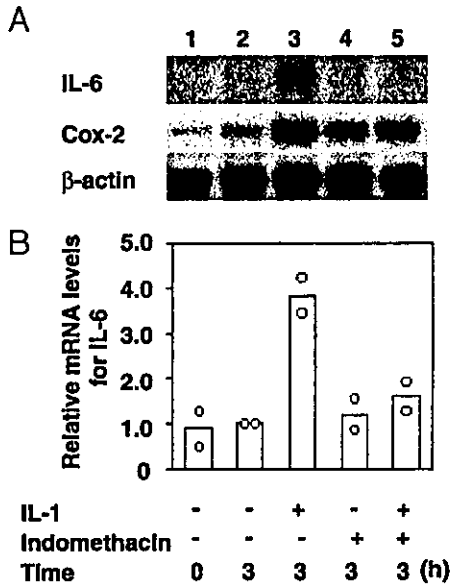

FIG. 3. The effect of indomethacin treatment on the expression of IL-6 after injection with IL-1α. Wild-type mice were treated with indomethacin 30 min before IL-1α injection and after 3 h; relative IL-6 mRNA levels in the diencephalon were analyzed by Northern blot hybridization. A, Northern blot hybridization profile. 1, nontreated mice; 2, 3 h after saline injection without pretreatment with indomethacin; 3, 3 h after IL-1 injection without pretreatment with indomethacin; 4, 3 h after saline injection with pretreatment with indomethacin; and 5, 3 h after IL-1 injection with pretreatment with indomethacin. mRNAs from four mice were used for each lane. B, Relative radioactivity of the bands corresponding to IL-6, normalized against the intensity of the *β-actin* bands. Similar results were obtained in another experiment.

increase in IL-1α and IL-1β mRNA levels in the diencephalon of the brain. These observations strongly suggested involvement of IL-1 in the brain in febrile response (8). In this report, however, we have shown that endogenous IL-1 in the brain is not necessary for the development of fever, because a febrile response was observed in *IL-1α/β*-deficient mice upon peripheral administration of IL-1α. Although this result does not necessarily exclude the possibility that endogenous IL-1 in the brain plays an important role in the febrile response in wild-type mice, it indicates that peripheral IL-1 can induce fever through mechanisms other than inducing *IL-1* in the brain inside the BBB.

We observed rather higher febrile response in *IL-1α/β*-deficient mice than in wild-type mice. This result is consistent with the hyperresponsive febrile reaction of *IL-1β*-deficient mice by ip injection of IL-1α, IL-1β, or LPS (10). The increased febrile response could be explained by the number or the affinity of IL-1Rs in *IL-1α/β*-deficient mice, although no such differences in IL-1Rs were reported in *IL-1β*-deficient mice (10). The hyperresponsive febrile response may also reflect lower levels of IL-1Ra in the brain. Consistent with this notion, we reported that IL-1Ra levels in the brain were decreased in IL-1α- or IL-1β-deficient mice (8).

Then, we analyzed the signal transduction mechanisms during febrile response in the brain. It has been reported that *Cox-2* is induced by IL-1 (19–22), that *Cox-2* null mutant mice failed to show a febrile response to IL-1β (15), and that various Cox-2 inhibitors including indomethacin suppress the development of fever upon inflammation (15), suggesting involvement of PGE_2 in IL-1-induced febrile response. Endogenously induced IL-6 has also been suggested to be involved in the febrile response induced by IL-1, because *IL-6* null mutant mice failed to mount a febrile response to peripherally injected IL-1β (16) or IL-1α (Fig. 1B). In this report, we have analyzed the relationship among IL-1, IL-6, and Cox-2, and demonstrated that: 1) *Cox-2* is strongly induced 1.5 h after iv injection of IL-1α, followed by *IL-6* at 3 h after injection; 2) *Cox-2* induction in the brain is not affected by deficiencies in IL-1 or IL-6; 3) no fever development is observed in *IL-6*-deficient mice, although *Cox-2* is induced in the brain; and 4) inhibition of Cox activity by indomethacin suppresses both *IL-6* induction and fever development. These results suggest the following signaling cascade in the febrile response: peripheral IL-1α → *Cox-2* activation in the brain → PGE_2 → *IL-6* induction → fever development. It has been well documented that IL-1 can induce *Cox-2* expression both *in vitro* and *in vivo* (19–21, 23). The endothelium of the cerebral vasculature may be the site where circulating IL-1 interacts with its receptors. Indeed, we and other investigators (4, 24) observed expression of IL-1RI on cerebral blood vessels after treatment with IL-1 (data not shown) (4, 24). Because *Cox-2* is induced in the microvessels of the brain upon IL-1 injection (24–26), PGE_2 may be released inside the brain through the BBB to induce IL-6 inside the brain. It was also suggested that IL-1 might penetrate the fenestrated endothelia of capillaries of organum vasculosum laminae terminalis, bind to their receptors located on astrocytes that tightly surround the vascular network, and trigger the synthesis and release of PGE_2 (5, 27).

There has been some confusion among data relating to the signaling cascade in the brain that occurs during inflammation. It was reported that intracerebroventricular injection of IL-6 induces an increase of PGE_2 levels in the cerebrospinal fluid in parallel with the rise in body temperature in cats (28), suggesting that IL-6 induces *Cox-2*. Another study has also demonstrated that PGE_2 release from rat hypothalamic explants is increased by both IL-1β and IL-6 *in vitro* (29). In contrast, this report shows that peripherally injected IL-1 can induce *Cox-2* in *IL-6*-deficient mice without fever development, and indomethacin inhibits *IL-6* induction, suggesting that *IL-6* is induced downstream of Cox-2. In support of this notion, several reports have demonstrated that *IL-6* is induced by PGE_2 in activated peritoneal macrophages (30, 31). The expression of *IL-6* in the brain has also been suggested to be downstream of PGE_2; one such study reported that hyperthermia induced by PGE_2 was markedly suppressed by the microinjection of anti-IL-6 directly into the anterior hypothalamic preoptic area (32). Furthermore, PGE_2 induces IL-6 in U373 MG human astroglioma cells (33), and inhibition of Cox-2 reduces IL-6 synthesis in human postmortem astrocyte cultures (34). Intravenous administration of IL-6, however, did not induce *Cox-2* expression in the rat brain. Thus, IL-6 may induce *Cox-2*, and *vice versa*, under artificial conditions, but only *IL-6* induction by PGE_2 appears to occur in the brain during an *in vivo* febrile response against IL-1α in mice.

It is known that IL-1α induces other cytokines such as IL-6 or TNFα in the periphery (35). IL-1 and TNFα synergistically increase the production of IL-6 in human synovial fibroblast (36). Thus, it is possible that the febrile response is not caused directly by IL-1α, but rather other cytokines that are induced by IL-1α in the periphery. Regarding this possibility, we could not detect any febrile response by the injection of IL-6 into wild-type mice, consistent with the previous observation (16). On the other hand, administration of TNFα could evoke febrile response in *IL-1α*-deficient mice as in wild-type mice. Thus, it is possible that the febrile response may actually be caused by other cytokines that are induced by IL-1α in the periphery.

Finally, we have shown that both early febrile response, which occurs during the 15–45 min after IL-1α administration, and late response, which occurs after 1 h 45 min, were abolished in *IL-6*-deficient mice. However, suppression of the early response is rather unexpected, because IL-6 induction was only low during the early phase. It is possible that only low levels of IL-6 are enough for the induction of fever. Consistent with our results, Chai *et al.* (16) reported that LPS- or IL-1β-induced fever response was completely abolished in *IL-6*-deficient mice, although the early response was not clear. However, because the early febrile response against IL-1α in mice was very small compared with that of rabbits or rats against LPS or IL-1β (5, 37), we might have failed to detect the response. We are now further analyzing the signaling mechanism of the early-phase febrile response.

In conclusion, we have shown that endogenous brain IL-1 is not necessary for IL-1-induced fever development. We suggest that the signaling cascade for the febrile response in the brain is as follows: peripheral IL-1α → *Cox-2* activation → PGE_2 → *IL-6* induction → fever. We are now analyzing the

roles of other cytokines in the brain in the development of fever.

Acknowledgments

Received January 19, 2004. Accepted July 12, 2004.

Address all correspondence and requests for reprints to: Yoichiro Iwakura, D.Sc., Professor, Center for Experimental Medicine, Institute of Medical Science, University of Tokyo, 4-6-1 Shirokanedai, Minato-ku, Tokyo 108-8639, Japan. E-mail: iwakura@ims.u-tokyo.ac.jp.

Current address for T.S.: Department of Developmental Physiology, National Institute for Physiological Sciences, Myodaiji, Okazaki 444-8585, Japan.

Current address for M.A.: Division of Transgenic Animal Science, Kanazawa University Advanced Science Research Center, 13-1 Takaramachi, Kanazawa 920-8640, Japan.

This work was supported by the grants from the Ministry of Education, Culture, Sports, Science and Technology of Japan, the Ministry of Health, Labor and Welfare of Japan, and Pioneering Research Project in Biotechnology.

References

1. **Dinarello CA** 1996 Biologic basis for interleukin-1 in disease. Blood 87:2095–2147
2. **Takao T, Tracey DE, Mitchell WM, De Souza EB** 1990 Interleukin-1 receptors in mouse brain: characterization and neuronal localization. Endocrinology 127:3070–3078
3. **French RA, VanHoy RW, Chizzonite R, Zachary JF, Dantzer R, Parnet P, Bluthe RM, Kelley KW** 1999 Expression and localization of p80 and p68 interleukin-1 receptor proteins in the brain of adult mice. J Neuroimmunol 93:194–202
4. **Ericsson A, Liu C, Hart RP, Sawchenko PE** 1995 Type 1 interleukin-1 receptor in the rat brain: distribution, regulation, and relationship to sites of IL-1-induced cellular activation. J Comp Neurol 361:681–698
5. **Kluger MJ** 1991 Fever: role of pyrogens and cryogens. Physiol Rev 71:93–127
6. **Rothwell NJ, Hopkins SJ** 1995 Cytokines and the nervous system II: actions and mechanisms of action. Trends Neurosci 18:130–136
7. **Engblom D, Ek M, Saha S, Ericsson-Dahlstrand A, Jakobsson PJ, Blomqvist A** 2002 Prostaglandins as inflammatory messengers across the blood-brain barrier. J Mol Med 80:5–15
8. **Horai R, Asano M, Sudo K, Kanuka H, Suzuki M, Nishihara M, Takahashi M, Iwakura Y** 1998 Production of mice deficient in genes for interleukin (IL)-1α, IL-1β, IL-1α/β, and IL-1 receptor antagonist shows that IL-1β is crucial in turpentine-induced fever development and glucocorticoid secretion. J Exp Med 187:1463–1475
9. **Leon LR, Conn CA, Glaccum M, Kluger MJ** 1996 IL-1 type I receptor mediates acute phase response to turpentine, but not lipopolysaccharide, in mice. Am J Physiol 271:R1668–R1675
10. **Alheim K, Chai Z, Fantuzzi G, Hasanvan H, Malinowsky D, Santo ED, Ghezzi P, Dinarello CA, Bartfai T** 1997 Hyperresponsive febrile reactions to interleukin (IL) 1α and IL-1β, and altered brain cytokine mRNA and serum cytokine levels, in IL-1β-deficient mice. Proc Natl Acad Sci USA 94:2681–2686
11. **Murakami N, Sakata Y, Watanabe T** 1990 Central action sites of interleukin-1β for inducing fever in rabbits. J Physiol 428:299–312
12. **Ushikubi F, Segi E, Sugimoto Y, Murata T, Matsuoka T, Kobayashi T, Hizaki H, Tuboi K, Katsuyama M, Ichikawa A, Tanaka T, Yoshida N, Narumiya S** 1998 Impaired febrile response in mice lacking the prostaglandin E receptor subtype EP3. Nature 395:281–284
13. **Smith WL, DeWitt DL, Garavito RM** 2000 Cyclooxygenases: structural, cellular, and molecular biology. Annu Rev Biochem 69:145–182
14. **Vane JR, Bakhle YS, Botting RM** 1998 Cyclooxygenases 1 and 2. Annu Rev Pharmacol Toxicol 38:97–120
15. **Li S, Ballou LR, Morham SG, Blatteis CM** 2001 Cyclooxygenase-2 mediates the febrile response of mice to interleukin-1β. Brain Res 910:163–173
16. **Chai Z, Gatti S, Toniatti C, Poli V, Bartfai T** 1996 Interleukin (IL)-6 gene expression in the central nervous system is necessary for fever response to lipopolysaccharide or IL-1β: a study on IL-6-deficient mice. J Exp Med 183: 311–316
17. **Kopf M, Baumann H, Freer G, Freudenberg M, Lamers M, Kishimoto T, Zinkernagel R, Bluethmann H, Kohler G** 1994 Impaired immune and acute-phase responses in interleukin-6-deficient mice. Nature 368:339–342
18. **Kozak W, Archuleta I, Mayfield KP, Kozak A, Rudolph K, Kluger MJ** 1998 Inhibitors of alternative pathways of arachidonate metabolism differentially affect fever in mice. Am J Physiol 275:R1031–R1040
19. **Ristimaki A, Garfinkel S, Wessendorf J, Maciag T, Hla T** 1994 Induction of cyclooxygenase-2 by interleukin-1α. Evidence for post-transcriptional regulation. J Biol Chem 269:11769–11775
20. **O'Banion MK, Miller JC, Chang JW, Kaplan MD, Coleman PD** 1996 Interleukin-1β induces prostaglandin G/H synthase-2 (cyclooxygenase-2) in primary murine astrocyte cultures. J Neurochem 66:2532–2540
21. **Samad TA, Moore KA, Sapirstein A, Billet S, Allchorne A, Poole S, Bonventre JV, Woolf CJ** 2001 Interleukin-1β-mediated induction of Cox-2 in the CNS contributes to inflammatory pain hypersensitivity. Nature 410:471–475
22. **Cao C, Matsumura K, Shirakawa N, Maeda M, Jikihara I, Kobayashi S, Watanabe Y** 2001 Pyrogenic cytokines injected into the rat cerebral ventricle induce cyclooxygenase-2 in brain endothelial cells and also upregulate their receptors. Eur J Neurosci 13:1781–1790
23. **Maier JA, Hla T, Maciag T** 1990 Cyclooxygenase is an immediate-early gene induced by interleukin-1 in human endothelial cells. J Biol Chem 265:10805–10808
24. **Ek M, Engblom D, Saha S, Blomqvist A, Jakobsson PJ, Ericsson-Dahlstrand A** 2001 Inflammatory response: pathway across the blood-brain barrier. Nature 410:430–431
25. **Cao C, Matsumura K, Yamagata K, Watanabe Y** 1996 Endothelial cells of the rat brain vasculature express cyclooxygenase-2 mRNA in response to systemic interleukin-1β: a possible site of prostaglandin synthesis responsible for fever. Brain Res 733:263–272
26. **Lacroix S, Rivest S** 1998 Effect of acute systemic inflammatory response and cytokines on the transcription of the genes encoding cyclooxygenase enzymes (COX-1 and COX-2) in the rat brain. J Neurochem 70:452–466
27. **Banks WA, Kastin AJ, Broadwell RD** 1995 Passage of cytokines across the blood-brain barrier. Neuroimmunomodulation 2:241–248
28. **Dinarello CA, Cannon JG, Mancilla J, Bishai I, Lees J, Coceani F** 1991 Interleukin-6 as an endogenous pyrogen: induction of prostaglandin E_2 in brain but not in peripheral blood mononuclear cells. Brain Res 562:199–206
29. **Navarra P, Pozzoli G, Brunetti L, Ragazzoni E, Besser M, Grossman A** 1992 Interleukin-1β and interleukin-6 specifically increase the release of prostaglandin E_2 from rat hypothalamic explants in vitro. Neuroendocrinology 56: 61–68
30. **Hinson RM, Williams JA, Shacter E** 1996 Elevated interleukin 6 is induced by prostaglandin E_2 in a murine model of inflammation: possible role of cyclooxygenase-2. Proc Natl Acad Sci USA 93:4885–4890
31. **Williams JA, Shacter E** 1997 Regulation of macrophage cytokine production by prostaglandin E_2. Distinct roles of cyclooxygenase-1 and -2. J Biol Chem 272:25693–25699
32. **Fernandez-Alonso A, Benamar K, Sancibrian M, Lopez-Valpuesta FJ, Minano FJ** 1996 Role of interleukin-1β, interleukin-6 and macrophage inflammatory protein-1β in prostaglandin-E_2-induced hyperthermia in rats. Life Sci 59:PL185–PL190
33. **Fiebich BL, Hull M, Lieb K, Gyufko K, Berger M, Bauer J** 1997 Prostaglandin E_2 induces interleukin-6 synthesis in human astrocytoma cells. J Neurochem 68:704–709
34. **Blom MA, van Twillert MG, de Vries SC, Engels F, Finch CE, Veerhuis R, Eikelenboom P** 1997 NSAIDS inhibit the IL-1β-induced IL-6 release from human post-mortem astrocytes: the involvement of prostaglandin E_2. Brain Res 777:210–218
35. **Nakae S, Komiyama Y, Narumi S, Sudo K, Horai R, Tagawa Y, Sekikawa K, Matsushima K, Asano M, Iwakura Y** 2003 IL-1-induced tumor necrosis factor-α elicits inflammatory cell infiltration in the skin by inducing IFN-γ-inducible protein 10 in the elicitation phase of the contact hypersensitivity response. Int Immunol 15:251–260
36. **Harigai M, Hara M, Kitani A, Norioka K, Hirose T, Hirose W, Suzuki K, Kawakami M, Masuda K, Shinmei M** 1991 Interleukin 1 and tumor necrosis factor-α synergistically increase the production of interleukin 6 in human synovial fibroblast. J Clin Lab Immunol 34:107–113
37. **Szekely M, Balasko M, Kulchitsky VA, Simons CT, Ivanov AI, Romanovsky AA** 2000 Multiple neural mechanisms of fever. Auton Neurosci 85:78–82

***Endocrinology* is published monthly by The Endocrine Society (http://www.endo-society.org), the foremost professional society serving the endocrine community.**

TNF-α is crucial for the development of autoimmune arthritis in IL-1 receptor antagonist–deficient mice

Reiko Horai,[1,2] Akiko Nakajima,[1] Katsuyoshi Habiro,[3] Motoko Kotani,[3] Susumu Nakae,[1] Taizo Matsuki,[1] Aya Nambu,[1] Shinobu Saijo,[1] Hayato Kotaki,[1] Katsuko Sudo,[1] Akihiko Okahara,[4] Hidetoshi Tanioka,[4] Toshimi Ikuse,[4] Naoto Ishii,[5] Pamela L. Schwartzberg,[2] Ryo Abe,[3] and Yoichiro Iwakura[1]

[1]Center for Experimental Medicine, Institute of Medical Science, University of Tokyo, Tokyo, Japan. [2]National Human Genome Research Institute, NIH, Bethesda, Maryland, USA. [3]Research Institute for Biological Sciences, Tokyo University of Science, Chiba, Japan. [4]Santen Pharmaceutical Co., Osaka, Japan. [5]Department of Microbiology and Immunology, Tohoku University Graduate School of Medicine, Sendai, Japan.

IL-1 receptor antagonist–deficient (IL-1Ra$^{-/-}$) mice spontaneously develop autoimmune arthritis. We demonstrate here that T cells are required for the induction of arthritis; T cell–deficient IL-1Ra$^{-/-}$ mice did not develop arthritis, and transfer of IL-1Ra$^{-/-}$ T cells induced arthritis in *nu/nu* mice. Development of arthritis was also markedly suppressed by TNF-α deficiency. We found that TNF-α induced OX40 expression on T cells and blocking the interaction between either CD40 and its ligand or OX40 and its ligand suppressed development of arthritis. These findings suggest that IL-1 receptor antagonist deficiency in T cells disrupts homeostasis of the immune system and that TNF-α plays an important role in activating T cells through induction of OX40.

Introduction

RA is a systemic, chronic, inflammatory disorder exhibited most commonly in the joints. Although various factors including genetic factors, environmental factors, and infectious agents have been suggested as causes of the disease (1), so far the etiology and pathogenesis have not been completely elucidated. Patients often produce autoantibodies against various self components such as IgGs, type II collagen, and nuclear antigens, suggesting an autoimmune nature of the disease (2). Many proinflammatory cytokines, including IL-1 and TNF-α, chemokines, and growth factors, are expressed in diseased joints, forming a complex cytokine network. It is widely believed that dysregulation of the cytokine network contributes to the pathogenesis of RA (3).

IL-1 is a prototype proinflammatory cytokine and is produced by various types of cells, including monocytes/macrophages, lymphocytes, and synovial lining cells (4). Since IL-1 induces inflammation, promotes synovial cell growth, and promotes differentiation of osteoclasts, an important role for this cytokine in the development of RA has been suggested (1, 5). IL-1 receptor antagonist (IL-1Ra) is an endogenous inhibitor of IL-1. IL-1Ra production is induced by a number of other cytokines, viral products, and acute-phase proteins and is augmented in patients with autoimmune and inflammatory diseases, suggesting that IL-1Ra may play regulatory roles in these diseases (6). TNF-α is also thought to be importantly involved in the inflammation and bone destruction in RA. TNF-α is produced mainly by monocytes/macrophages, which are activated by soluble components of bacteria and by direct contact with activated T cells at inflammatory sites. The production of IL-1 is coordinated with that of TNF-α, and they mutually stimulate each other's production. Overproduction of these cytokines by gene manipulation has been found to predispose the organism to inflammatory arthritis (7–10).

Cumulative evidence suggests that T cell–mediated autoimmune responses play a crucial role in the pathogenesis of RA. In fact, it has been demonstrated that T cells from RA patients can cause inflammatory arthritis in SCID mice (11). T cells that invade tissues and cause autoimmune destruction express activation antigens that are not expressed on normal resting T cells. These activation antigens include the IL-2 receptor α (CD25), CD69, CD44, CD40 ligand (CD40L; also known as CD154), and OX40 (also known as CD134) (12) CD40L on T cells and its receptor on APCs, as well as OX40 on T cells and its ligand (OX40L) on APCs, generate costimulatory signals that enhance T cell proliferation and cytokine production. Indeed, the expression of OX40 on T cells in rheumatoid synovial tissues is quite pronounced in some patients (12), and blocking either CD40L or OX40L in vivo reduces the severity of collagen-induced arthritis (CIA), experimental allergic encephalomyelitis, and inflammatory bowel disease in animal models of these diseases (13, 14). However, the molecular mechanisms for the induction of these costimulatory molecules in RA are not fully understood. We previously reported that IL-1 plays an important role in enhancing T cell–APC interactions through induction of CD40L and OX40 on T cells (15). Thus, excess IL-1 signaling may activate these pathways, leading to the development of T cell–mediated autoimmune diseases.

We previously reported that IL-1Ra$^{-/-}$ mice on the BALB/c background spontaneously develop chronic inflammatory arthropathy (9). Histopathology showed marked synovial and periarticular inflammation, with articular erosion caused by invasion of granulation tissues closely resembling that of RA in humans. Moreover, elevated levels of antibodies against immunoglobulins (rheumatoid factor [RF]), type II collagen, and double-stranded DNA were detected in sera of these mice, consistent with the development

Nonstandard abbreviations used: CD40L, CD40 ligand; CIA, collagen-induced arthritis; IL-1Ra, IL-1 receptor antagonist; PEC, peritoneal exudate cells; RF, rheumatoid factor.

Conflict of interest: The authors have declared that no conflict of interest exists.

Citation for this article: *J. Clin. Invest.* 114:1603–1611 (2004). doi:10.1172/JCI200420742.

Table 1
Incidence of arthritis in IL-1Ra$^{-/-}$ *scid/scid* mice

Genotype of *scid* loci	Incidence (%)
scid/scid	0/6 (0%)[A]
scid/+	9/11 (82%)
+/+	7/8 (88%)

Incidence of arthritis was judged at 20 weeks of age. Development of arthritis was completely suppressed in T cell–deficient IL-1Ra$^{-/-}$ *scid/scid* mice. [A]$P < 0.01$ by chi-square for independence test.

of autoimmunity. Proinflammatory cytokines such as IL-1β, IL-6, and TNF-α were overexpressed in the joints, indicating regulatory roles of IL-1Ra in the cytokine network. These data therefore suggested that IL-1Ra is crucial for the homeostasis of the immune system. It is not known, however, which cells in the immune system are crucial for the regulation of IL-1 and its actions, or furthermore, which cytokines are involved in the pathogenesis of arthritis in this model.

In this study, to elucidate the pathogenesis of the autoimmune arthritis in IL-1Ra$^{-/-}$ mice, we assessed the role of T cells in the development of arthritis by transferring T cells from IL-1Ra$^{-/-}$ mice to *nu/nu* mice and by intercrossing IL-1Ra$^{-/-}$ mice with T cell–deficient mice. We show that IL-1Ra$^{-/-}$ deficiency in T cells is enough for the development of arthritis. Furthermore, we analyzed the role of TNF-α in this model by producing TNF-α$^{-/-}$ IL-1Ra$^{-/-}$ mice, and we were able to demonstrate that TNF-α is crucial for the development of arthritis, as it induces OX40 on T cells. Treatment with anti-CD40L or anti-OX40L Ab suppressed disease, demonstrating the importance of CD40-CD40L and OX40-OX40L interactions for the development of autoimmune arthritis.

Results

Development of arthritis is suppressed in T cell– and B cell–deficient IL-1Ra$^{-/-}$ mice. IL-1Ra$^{-/-}$ mice on the BALB/c background spontaneously developed chronic inflammatory arthritis. Since high levels of RF, antibody to type II collagen, and antibody to double-stranded DNA are observed in IL-1Ra$^{-/-}$ mice, we hypothesized that there could be an autoimmune mechanism for the pathogenesis. To address this question, we evaluated the contribution of T cells and/or B cells to the development of arthritis in IL-1Ra$^{-/-}$ mice by intercrossing them with *scid/scid* mice on the BALB/c background. While IL-1Ra$^{-/-}$ *scid/+* or IL-1Ra$^{-/-}$ *+/+* mice showed a high incidence of arthritis, IL-1Ra$^{-/-}$ *scid/scid* mice failed to develop arthritis by 20 weeks of age (Table 1). These results suggest that combined deficiency of T and B cells completely suppresses the development of arthritis in IL-1Ra$^{-/-}$ mice.

Peripheral T cells from IL-1Ra$^{-/-}$ mice induced arthritis. We next examined the contribution of the specific cell types of the immune system to the development of arthritis by cell transfer experiments. When total splenocytes from IL-1Ra$^{-/-}$ mice were transferred into *nu/nu* mice on the BALB/c background, these mice developed severe arthritis as early as 3 weeks after the cell transfer (Figure 1, A and B). On the other hand, when T cell–depleted splenocytes were transferred into *nu/nu* mice, these mice did not develop arthritis at all. These results strongly suggest that T cells are involved in the development of arthritis. We further examined the effects of transplantation of purified T cells in the periphery. When T cells from spleens and LNs were transferred into *nu/nu* mice, they developed severe arthritis as early as 2 weeks after transfer (Figure 1, C and D). The disease status of the donor mice influenced these results; T cells from arthritic mice were more efficient than those

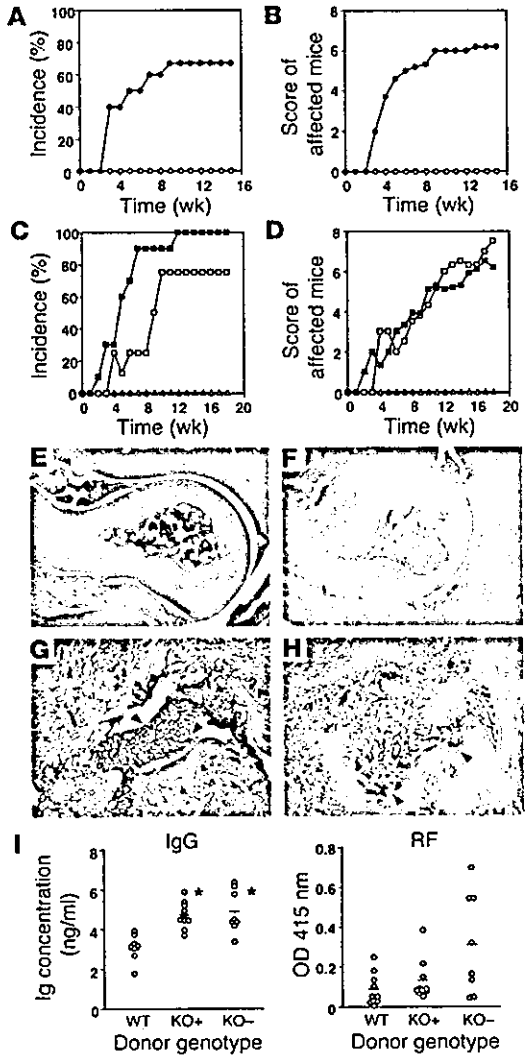

Figure 1
Splenocyte and T cell transfer into *nu/nu* mice. (**A**) Total splenocytes from IL-1Ra$^{-/-}$ mice (filled circles, $n = 10$) induced arthritis, while T cell–depleted splenocytes (open circles, $n = 7$) did not induce arthritis in *nu/nu* mice. (**B**) Arthritic severity score of splenocyte-transferred mice. (**C**) Purified T cells from spleen and LNs of either arthritic (filled squares, $n = 10$) or nonarthritic (open squares, $n = 8$) IL-1Ra$^{-/-}$ mice induced arthritis in *nu/nu* mice, while T cells from WT mice (triangles, $n = 11$) did not. (**D**) Arthritic severity score of T cell–transferred mice. (**E–H**) Histology of the ankle joints of WT (**E**) or IL-1Ra$^{-/-}$ (**F–H**) T cell–transferred *nu/nu* mice. (**G**) Infiltration of inflammatory cells (indicated by arrowheads). (**H**) Erosive bone destruction by replacement of bone matrix with fibroblastic cells (indicated by arrowheads). Magnification, ×40 (**E** and **F**); ×100 (**G** and **H**). (**I**) Serum IgG (left) and RF (right) levels in WT T cell– or IL-1Ra$^{-/-}$ T cell–transferred *nu/nu* mice. The average in each group is shown as a horizontal bar. WT, WT donors ($n = 10$); KO+, arthritic-IL-1Ra$^{-/-}$ donors ($n = 10$); KO–, nonarthritic IL-1Ra$^{-/-}$ donors ($n = 8$). $^*P < 0.05$.

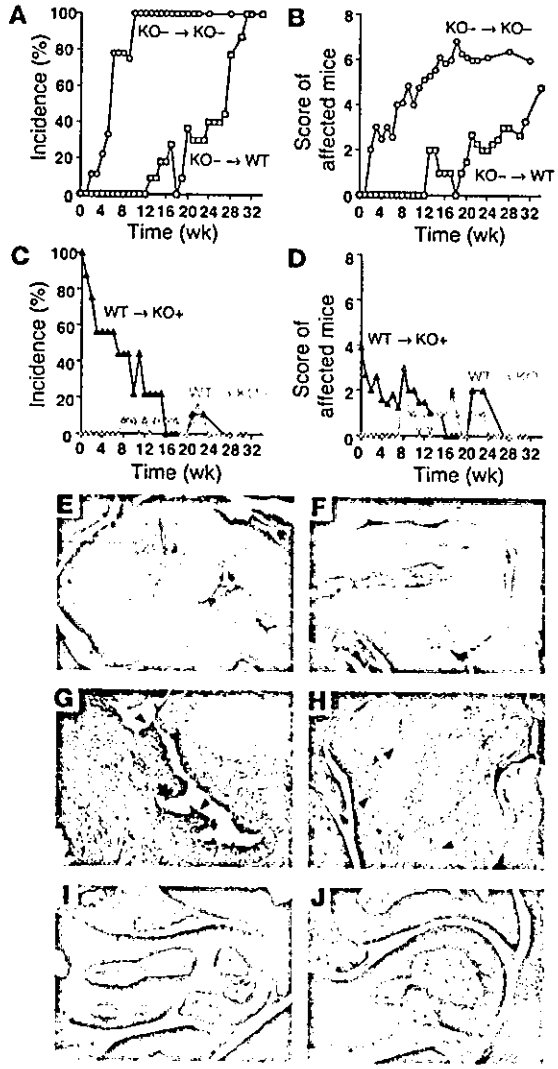

Figure 2
BM cell replacement between WT and IL-1Ra$^{-/-}$ mice. BM cells from IL-1Ra$^{-/-}$ mice induced arthritis in WT mice, while those from WT mice suppressed arthritis in IL-1Ra$^{-/-}$ mice. (**A**) Incidence of arthritis in IL-1Ra$^{-/-}$ BM cell–transferred WT (squares, $n = 11$) or IL-1Ra$^{-/-}$ mice (circles, $n = 9$). (**B**) Arthritic severity score of IL-1Ra$^{-/-}$ BM cell–transferred mice. (**C**) Incidence of arthritis in WT BM cell–transferred IL-1Ra$^{-/-}$ mice with (closed triangle, $n = 9$) or without (open triangle, $n = 13$) arthritis. (**D**) Arthritic severity score of WT BM–transferred IL-1Ra$^{-/-}$ mice. (**E–H**) Histopathology of the ankle joints of IL-1Ra$^{-/-}$ BM cell–transferred IL-1Ra$^{-/-}$ mice (**E**) and IL-1Ra$^{-/-}$ BM cell–transferred WT mice (**F–H**) at the end of the experiments (32 weeks and 34 weeks after the cell transfer, respectively). (**G**) Infiltration of inflammatory cells (indicated by arrowheads) into articular space and proliferation of the lining cells of the synovial membrane. (**H**) Pannus formation and erosive destruction of the bone (indicated by arrowheads). (**I** and **J**) Histology of the normal ankle joints of WT BM cell–transferred nonarthritic IL-1Ra$^{-/-}$ mice (**I**) and arthritic IL-1Ra$^{-/-}$ mice (**J**) at 31 weeks after the cell transfer. Magnification, ×40 (**E**, **F**, **I**, and **J**); ×100 (**G** and **H**).

from nonarthritic mice in inducing arthritis in recipient mice (Figure 1C). However, cells from both arthritic and nonarthritic mice could induce the disease. Histological analyses revealed that arthritis was observed in both ankle and knee joints of IL-1Ra$^{-/-}$ T cell–transferred *nu/nu* mice (Figure 1, F–H and data not shown). Proliferation of synovial cells, infiltration of neutrophils and lymphocytes, and bone destruction were remarkable in both ankle and knee joints (Figure 1, E–H and data not shown). Serum IgG levels and RF levels were enhanced in IL-1Ra$^{-/-}$ T cell–transferred *nu/nu* mice compared with WT T cell–transferred mice, although the difference in RF levels was not statistically significant (Figure 1I). We also performed thymocyte transfer experiments to examine whether or not activation of IL-1Ra$^{-/-}$ T cells before transplantation is necessary, and we found that thymocytes from IL-1Ra$^{-/-}$ mice induced arthritis in *nu/nu* mice, but with lower frequency than that seen in mice transferred with splenocytes or purified T cells (IL-1Ra$^{-/-}$ thymocyte–transferred mice, 46%; WT thymocyte–transferred mice, 0% at 15 weeks). These results clearly indicate that T cells are required for the development of arthritis in IL-1Ra$^{-/-}$ mice, and suggest that IL-1Ra$^{-/-}$ T cells can enhance immune responses against self components.

BM-derived cells from IL-1Ra$^{-/-}$ mice induced arthritis in normal mice and those from normal mice suppressed the development of arthritis in IL-1Ra$^{-/-}$ mice. To examine whether abnormal T cell education or a stem cell disorder is responsible for the T cell abnormality seen in IL-1Ra$^{-/-}$ mice, we next reconstituted the immune system by BM cell transfers. BM cells were prepared from IL-1Ra$^{-/-}$ mice by treating these cells with anti-Thy-1.2 Ab to deplete T cells, and then they were transferred into the recipient mice that were lethally irradiated. Mice that received BM cells did not die, whereas those that did not receive BM cells died within 2 weeks. We observed the development of arthritis as early as 2 weeks after the transfer of 4-week-old IL-1Ra$^{-/-}$ BM cells to nonarthritic IL-1Ra$^{-/-}$ mice, which would normally develop arthritis at 5–8 weeks of age (Figure 2A). Arthritis was also observed in WT mice receiving IL-1Ra$^{-/-}$ BM cells. These mice developed arthritis, however, more than 3 months after the transfer, indicating that the genotype of recipient mice (WT or IL-1Ra–deficient) affects the incidence and severity of arthritis (Figure 2, A and B). Replacement of the recipient BM cells by the donor cells was confirmed by Southern blot analyses at the end of the experiments. Cells from lymphoid tissues such as the spleen and LNs consisted mainly of the donor cells, while those from joints showed both donor and recipient genotypes (data not shown), suggesting that only BM-derived cells were replaced in the joints (16). Histological analysis of the ankle joints showed synovial and periarticular inflammation with articular erosion in both WT and IL-1Ra$^{-/-}$ mice that received IL-1Ra$^{-/-}$ BM cells (Figure 2, E and F). We observed proliferation of synovial lining cells and invasion of inflammatory cells, includ-

Table 2
Increased cytokine secretion by CD4$^+$ T cells from IL-1Ra$^{-/-}$ mice

Cytokine	Detection limit	WT	IL-1Ra$^{-/-}$
IFN-γ (U/ml)	20 U/ml	59.7 ± 13.0	153.8 ± 19.1^A
IL-4 (pg/ml)	10 pg/ml	42.0 ± 5.0	161.9 ± 3.2^A
TNF-α (pg/ml)	12.5 pg/ml	52.0 ± 7.8	95.3 ± 3.7^A

Purified CD4$^+$ T cells were stimulated with 1 μg/ml (IFN-γ and IL-4) or 10 μg/ml (TNF-α) of plate-coated anti-CD3 mAb for 48 hours. Data are expressed as mean ± SEM ($n = 4$). $^AP < 0.01$ by Student's t test. Similar results were obtained from 2 independent experiments.

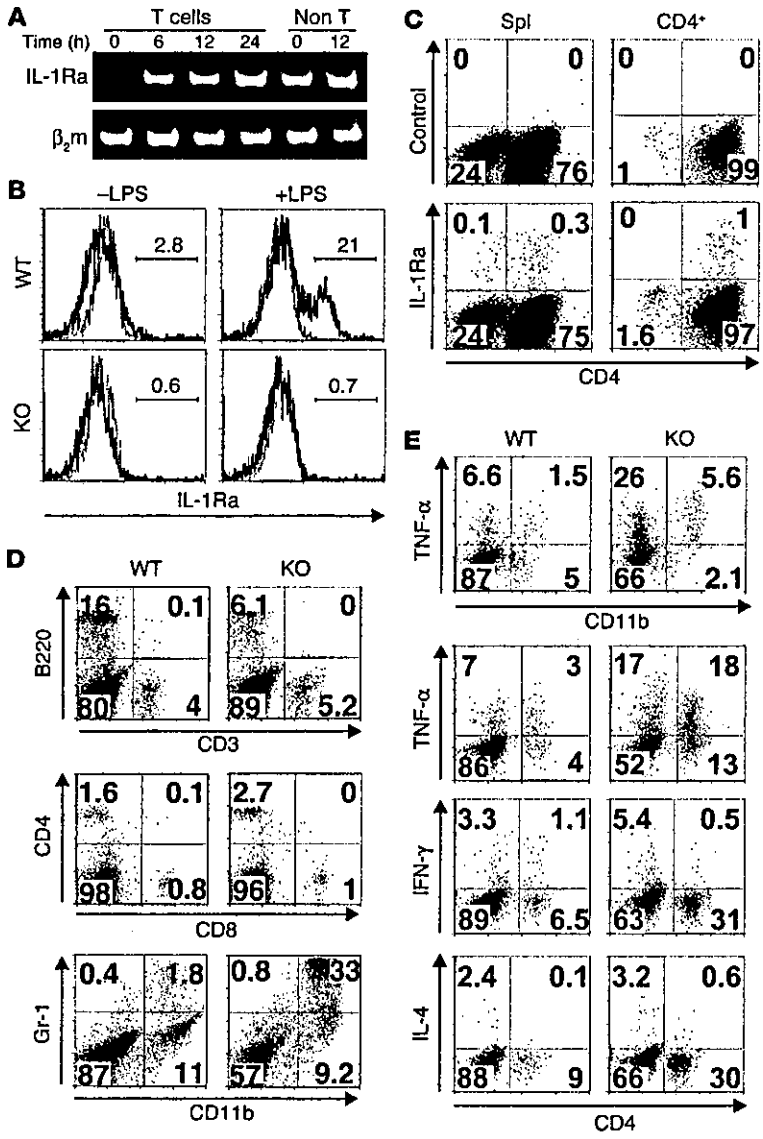

Figure 3
IL-1Ra and cytokine production. (**A**) *IL-1Ra* mRNA expression in WT T cells. Purified T cells from WT mice were stimulated with 10 μg/ml of plate-coated anti-CD3 mAb for 0, 6, 12, or 24 hours, and *IL-1Ra* mRNA levels were determined by RT-PCR. T cell–depleted splenocytes (Non T) were stimulated with 5 μg/ml LPS for 0 and 12 hours as controls. β_2m is used as an internal control. (**B**) Intracellular staining for IL-1Ra in PECs. PECs from WT and IL-1Ra$^{-/-}$ mice were stimulated with LPS, and IL-1Ra$^+$ cells in the CD11b$^+$ population are shown as histograms. Black-lined histograms: staining with IL-1Ra Ab. Gray-lined histograms: staining with isotype control Ig. Percentages of IL-1Ra$^+$ cells are indicated. (**C**) Intracellular staining for IL-1Ra in splenocytes (Spl) and CD4$^+$ T cells from WT mice after stimulation with anti-CD3 mAb. Upper panels show staining with isotype control Ig and lower panels show staining with anti–IL-1Ra Ab. (**D**) Expression of cell lineage–specific surface molecules on cells from ankle joints of WT and IL-1Ra$^{-/-}$ (KO) mice. B220, Gr-1, and CD11b are markers for B cells, granulocytes (including neutrophils), and macrophages, respectively. (**E**) Intracellular staining for cytokines in cells from the ankle joints of WT and IL-1Ra$^{-/-}$ mice. Joint-derived cells were stimulated with 10 ng/ml PMA and 400 ng/ml ionomycin for 6 hours with 2 μM monensin. Similar results were obtained in 3 independent experiments.

ing lymphocytes and neutrophils (Figure 2, E–G). Bone erosion and pannus formation were also remarkable (Figure 2H).

To examine whether normal stem cells can suppress the development of arthritis in IL-1Ra$^{-/-}$ mice, we prepared BM cells from WT mice and transferred them into irradiated nonarthritic or arthritic IL-1Ra$^{-/-}$ mice. Development of arthritis was suppressed in nonarthritic IL-1Ra$^{-/-}$ mice that received normal BM cells (Figure 2, C and D). Arthritis was also ameliorated in arthritic IL-1Ra$^{-/-}$ mice that received normal BM cells (Figure 2, C and D). At 31 weeks after transfer of BM cells, joint pathology was examined histologically. Nonarthritic IL-1Ra$^{-/-}$ mice that received normal BM cells showed no sign of arthritis (Figure 2I). Moreover, arthritic IL-1Ra$^{-/-}$ mice that received normal BM cells showed complete recovery from arthritis (Figure 2J). Thus, replacement of the BM-derived cells in IL-1Ra$^{-/-}$ mice with those of normal mice can suppress and actually reverse the development of arthritis in IL-1Ra$^{-/-}$ mice. These results indicate that BM-derived cells themselves are abnormal in IL-1Ra$^{-/-}$ mice.

Enhanced cytokine production from activated T cells in IL-1Ra$^{-/-}$ mice. Since our results suggested abnormal T cell function in IL-1Ra$^{-/-}$ mice, we next analyzed T cell proliferation and cytokine production upon TCR stimulation. Proliferative responses of T cells from IL-1Ra$^{-/-}$ mice stimulated with anti-CD3 mAb were normal (data not shown). However, these T cells produced much higher levels of IFN-γ, IL-4, and TNF-α in the culture supernatant than did those from WT mice (Table 2). These results suggest that IL-1Ra$^{-/-}$ T cells produce higher levels of cytokines upon TCR stimulation.

We also examined IL-1Ra expression in normal WT T cells by RT-PCR, ELISA, and intracellular staining. Unstimulated T cells expressed low levels of *IL-1Ra* mRNA, but upon stimulation through TCR, *IL-1Ra* mRNA expression was upregulated (Figure 3A). We also observed secretion of the IL-1Ra protein in the culture supernatant of WT purified CD4$^+$ T cells (>99% purity) after anti-CD3 mAb stimulation (20–40 pg/ml at 72–96 hours), indicating that T cells can produce and secrete the IL-1Ra protein. To confirm the IL-1Ra protein production from T cells directly, we stained stimulated CD4$^+$ T cells intracellularly with anti-IL-1Ra Ab. As a control experiment for the staining, we first stained peritoneal exudate cells (PECs) from WT or IL-1Ra$^{-/-}$ mice stimulated with or without LPS, and showed that the staining specifically detected IL-1Ra after the stimulation (Figure 3B). Then, purified CD4$^+$ T cells from BALB/c WT mice were stimulated with plate-coated anti-CD3 mAb and stained for the intracellular IL-1Ra protein. As shown in Figure 3C, CD4$^+$ T cells can produce IL-1Ra protein after TCR stimulation. These IL-1Ra–producing cells were different from those which produce IFN-γ, IL-4, or IL-10 under these conditions (data not shown). These results indicate that IL-1Ra is produced by T cells and may regulate T cell activation by IL-1.

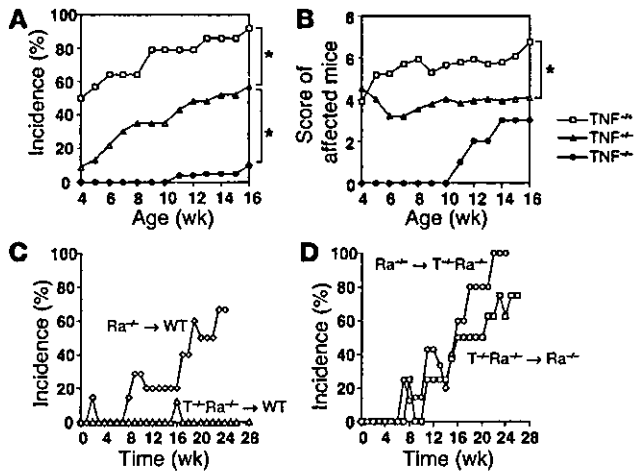

Figure 4

Incidence of arthritis in TNF-α–deficient IL-1Ra$^{-/-}$ mice. Incidence (**A**) and severity score (**B**) of arthritis in TNF-α–deficient IL-1Ra$^{-/-}$ mice. Squares, TNF-α$^{+/+}$ IL-1Ra$^{-/-}$ mice (n = 14); triangles, TNF-α$^{+/-}$ IL-1Ra$^{-/-}$ mice (n = 23); circles, TNF-α$^{-/-}$ IL-1Ra$^{-/-}$ mice (n = 23). Statistical significance between genotypes was calculated by repeated-measures ANOVA or two-way ANOVA. *P < 0.01. (**C**) Incidence of arthritis in TNF-α$^{-/-}$ IL-1Ra$^{-/-}$ (Ra$^{-/-}$) or IL-1Ra$^{-/-}$ BM cell–transferred WT mice. Triangles, WT mice transferred with TNF-α$^{-/-}$ IL-1Ra$^{-/-}$ BM cells (T$^{-/-}$Ra$^{-/-}$ → WT); diamonds, WT or heterozygous (IL-1Ra$^{+/-}$) mice transferred with IL-1Ra$^{-/-}$ BM cells (Ra$^{-/-}$ → WT). (**D**) Incidence of arthritis in TNF-α$^{-/-}$ IL-1Ra$^{-/-}$ or IL-1Ra$^{-/-}$ BM cell–transferred IL-1Ra$^{-/-}$ mice. Squares, IL-1Ra$^{-/-}$ mice transferred with TNF-α$^{-/-}$ IL-1Ra$^{-/-}$ BM cells (T$^{-/-}$Ra$^{-/-}$ → Ra$^{-/-}$); circles, TNF-α$^{-/-}$ IL-1Ra$^{-/-}$ mice transferred with IL-1Ra$^{-/-}$ BM cells (Ra$^{-/-}$ → T$^{-/-}$Ra$^{-/-}$).

Identification of cells in the joints and cellular cytokine production. To further analyze the roles of cytokines overexpressed in IL-1Ra$^{-/-}$ T cells, we examined the local subsets of lymphocytes and their cytokine production in the joints. The ankle joints were dissected, and cytokine production in the joint cells was examined by intracellular staining. The total cell number in the ankle joints was increased 2-fold in IL-1Ra$^{-/-}$ mice (7.1×10^6 cells per mouse, n = 10) compared to WT mice (3.7×10^6 cells per mouse, n = 10), suggesting infiltration of inflammatory cells. Thus, although the proportion of T cells was not dramatically increased (Figure 3D), the total T cell numbers in the joints of IL-1Ra$^{-/-}$ mice were greater than in WT mice. In the T lymphocyte subsets, CD4$^+$ cells were detected more frequently than CD8$^+$ cells, consistent with our previous observations (17). We also observed increased infiltration of CD11b$^+$ Gr-1$^+$ cells, most likely activated neutrophils, in the arthritic joints of IL-1Ra$^{-/-}$ mice (Figure 3D).

Cells from the ankle joints were stimulated with PMA and ionomycin to examine the ability to produce cytokines such as TNF-α, IFN-γ, and IL-4. As shown in Figure 3E, most of the IL-1Ra$^{-/-}$ CD11b$^+$ cells produced TNF-α. Some of CD4$^+$ T cells in the joints were also TNF-α–producing cells. Moreover, many more of these cells were found in the IL-1Ra$^{-/-}$ joints, suggesting that the infiltrating CD4$^+$ T cells in arthritic joints may produce more TNF-α and enhance inflammation. Only a small percentage of cells in the joints produced IFN-γ or IL-4 in either WT mice or IL-1Ra$^{-/-}$ mice.

Suppression of arthritis in TNF-α–deficient IL-1Ra$^{-/-}$ mice. We previously reported that high levels of inflammatory cytokines, including TNF-α, were detected in the joints of IL-1Ra$^{-/-}$ mice (9). We also observed TNF-α–producing cells in the ankle joints of these mice (Figure 3E). Furthermore, we detected high levels of TNF-α in the culture of IL-1Ra$^{-/-}$ T cells (Table 2). To elucidate the role of TNF-α in the development of arthritis in IL-1Ra$^{-/-}$ mice, we generated TNF-α and IL-1Ra double-deficient mice by crossing IL-1Ra$^{-/-}$ mice with TNF-α$^{-/-}$ mice.

As shown in Figure 4, A and B, homozygous TNF-α deficiency strongly suppressed development of arthritis in IL-1Ra$^{-/-}$ mice. An intermediate, but significant, suppression was observed in mice heterozygous for the *TNF-α* gene, suggesting a *TNF-α* gene dosage effect on the incidence and severity of arthritis. Histological analyses revealed that TNF-α$^{-/-}$ IL-1Ra$^{-/-}$ mice that appeared normal also showed normal joint histology, but those with swollen joints showed arthritic pathology of inflammation and bone destruction similar to that seen in IL-1Ra$^{-/-}$ mice (data not shown). These results suggest that TNF-α plays critical roles in the development of arthritis in IL-1Ra$^{-/-}$ mice.

However, since the *TNF-α* gene is located in the MHC locus and mice deficient for this gene were produced on the 129 background (H-2^b), TNF-α$^{-/-}$ mice backcrossed to the BALB/c strain (H-2^d) for 8 generations still had the same H-2 locus as the 129 mice. To examine the contribution of the MHC locus in the development of arthritis in IL-1Ra$^{-/-}$ mice, IL-1Ra$^{-/-}$ mice were crossed with the BALB.B congenic for the C57BL/6 H-2 locus (H-2^b) or the B10.D2/n congenic for the BALB/c H-2 locus. The results clearly argued that MHC differences were not responsible for the suppression of arthritis in TNF-α$^{-/-}$ mice (data not shown).

To further analyze the role of TNF-α in the development of arthritis in IL-1Ra$^{-/-}$ mice, we examined the effects of TNF-α deficiency in BM cell transfer experiments. BM cells from TNF-α$^{-/-}$ IL-1Ra$^{-/-}$ mice did not induce arthritis in WT mice up to 30 weeks after transfer, while BM cells from IL-1Ra$^{-/-}$ mice induced arthritis in WT mice starting after 8 to 12 weeks (Figures 2A and 4C). On the other hand, TNF-α$^{-/-}$ IL-1Ra$^{-/-}$ BM cells transferred into IL-1Ra$^{-/-}$ mice induced arthritis, and IL-1Ra$^{-/-}$ BM cells transferred into TNF-α$^{-/-}$ IL-1Ra$^{-/-}$ mice also induced arthritis (Figure 4, C and D). These results suggest that TNF-α produced by both BM-derived cells and non-BM-derived cells plays an important role in the development of arthritis

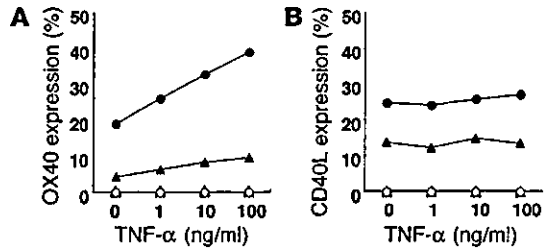

Figure 5

Induction of OX40 expression on T cells by TNF-α. (**A**) OX40 expression (%) on CD4$^+$ T cells stimulated with plate-coated anti-CD3 mAb (0.1 or 0.3 μg/ml) plus TNF-α (0, 1, 10, or 100 ng/ml) for 72 hours. Open symbols: control Ig staining. Filled symbols: anti-OX40 Ab staining for 0.1 μg/ml (triangles) or 0.3 μg/ml (circles) of anti-CD3 mAb stimulation. (**B**) CD40L expression (%) on CD4$^+$ T cells stimulated with plate-coated anti-CD3 mAb (0.1 or 0.3 μg/ml) plus TNF-α (0, 1, 10, or 100 ng/ml) for 24 hours. Open symbols: control Ig staining. Filled symbols: anti-OX40 Ab staining for 0.1 μg/ml (triangles) or 0.3 μg/ml (circles) of anti-CD3 mAb stimulation. Similar results were obtained in 5 independent experiments.

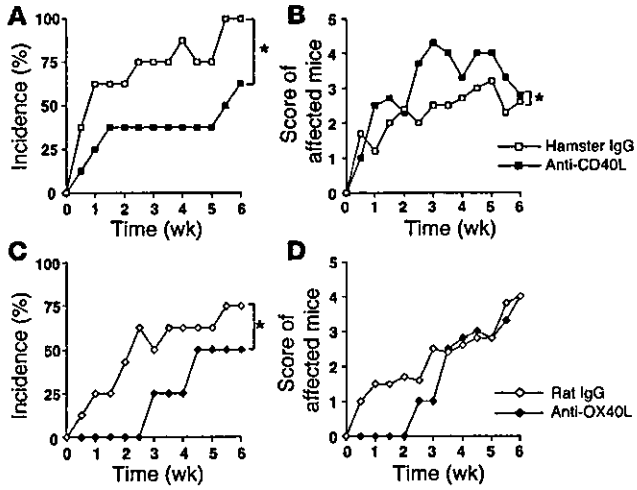

Figure 6
Anti-CD40L or anti-OX40L Ab treatment of IL-1Ra$^{-/-}$ mice. Blocking Abs against either CD40L or OX40L were administrated to IL-1Ra$^{-/-}$ mice before the onset of arthritis. Ab treatment was continued twice a week for 6 weeks, and incidence of arthritis was inspected each time before Ab administration. Incidence and severity score of arthritis in control hamster IgG–treated (open squares, $n = 8$) or anti-CD40L Ab–treated (filled squares, $n = 8$) IL-1Ra$^{-/-}$ mice (**A** and **B**) and those in control rat IgG–treated (open diamonds, $n = 8$) or anti-OX40L Ab–treated (closed diamonds, $n = 8$) IL-1Ra$^{-/-}$ mice (**C** and **D**). *$P < 0.01$ by repeated-measures ANOVA or 2-way ANOVA.

in IL-1Ra$^{-/-}$ mice. Since TNF-α is crucial for the development of arthritis in this model, these results suggest that TNF-α can be produced in the IL-1Ra$^{-/-}$ recipient mice from relatively γ-ray–resistant cells such as macrophages or type A synovial cells.

TNF-α induced expression of OX40, but not CD40L, on T cells. We recently showed that IL-1 produced by APCs induces CD40L and OX40 expression on T cells (15). It has also been reported that ligation between CD40 on APCs and CD40L on T cells leads to TNF-α production from APCs (13). Here we examined the possible involvement of TNF-α in the induction of CD40L and OX40 on T cells. When CD4$^+$ T cells from WT mice were stimulated with varying concentrations of TNF-α (1–100 ng/ml) together with plate-coated anti-CD3 mAb (0–1 μg/ml), the higher concentrations of TNF-α upregulated OX40 expression (Figure 5A), but not CD40L expression, on T cells (Figure 5B). These results suggest that TNF-α may contribute to the development of arthritis in IL-1Ra$^{-/-}$ mice through the induction of OX40 expression on T cells. However, at the highest concentration of anti-CD3 mAb (1 μg/ml), maximal expression of OX40 could occur independent of TNF-α (data not shown).

Involvement of CD40-CD40L and/or OX40-OX40L pathways in the development of arthritis. To explore the contribution of CD40-CD40L and OX40-OX40L pathways to the pathogenesis of arthritis, we injected blocking Abs for these molecules into IL-1Ra$^{-/-}$ mice. Abs for either CD40L or OX40L were injected into IL-1Ra$^{-/-}$ mice for 6 weeks, starting from before onset of the disease, and incidence of arthritis was monitored during the administration period. As shown in Figure 6, Abs for both CD40L and OX40L were able to partially suppress development of arthritis in IL-1Ra$^{-/-}$ mice. The incidence of arthritis was lower in mice treated with anti-CD40L Ab than in those treated with control Ab (hamster IgG) (Figure 6A). The induction of arthritis was delayed in mice treated with anti-OX40L Ab, and the incidence of arthritis after 6 weeks was lower than in mice treated with control Ab (rat IgG) (Figure 6C). However, once arthritis was induced, antibody treatment was ineffective. The severity score of affected mice was similar in anti-OX40L–treated mice and control Ab–treated mice, and severity was actually exacerbated in mice treated with anti-CD40L Ab (Figure 6, B and D). Thus, these results suggest that both the CD40-CD40L and OX40-OX40L pathways are involved in development of arthritis in IL-1Ra$^{-/-}$ mice.

Discussion

In this study, we have shown that the development of arthritis in IL-1Ra$^{-/-}$ mice is completely suppressed in *scid/scid* mice and that IL-1Ra$^{-/-}$ T cell transfers induce arthritis in *nu/nu* mice, suggesting a crucial role of T cells in the pathogenesis of arthritis in this model (Table 1 and Figure 1). T cells from arthritic IL-1Ra$^{-/-}$ mice induced arthritis more efficiently than those from nonarthritic mice, suggesting that arthritogenic-activated and/or memory T cells are generated in IL-1Ra$^{-/-}$ mice and involved in the development of arthritis. However, cells from both arthritic and nonarthritic IL-1Ra$^{-/-}$ mice were able to induce arthritis, supporting a T cell intrinsic defect. Interestingly, donor T cells from IL-1Ra$^{-/-}$ mice are not necessarily primed by autoantigens, because naive T cells from thymus could induce arthritis, although this took longer than with peripheral T cells that may have been preactivated. With regard to this, we have previously shown that IL-1 from APCs can activate T cells through the induction of CD40L and OX40 on T cells (15), and in the absence of IL-1Ra, even physiological levels of IL-1 activate T cells excessively, resulting in the development of autoimmunity (9). Our present data suggest that T cell–derived IL-1Ra also regulates T cell activity in an autocrine manner, although IL-1Ra is known to be produced by many other types of cells, including monocytes and macrophages in the synovial lining layer. In support of this notion, *IL-1Ra* mRNA expression was observed in unstimulated T cells at low levels but stronger expression was induced in activated T cells (Figure 3A). Thus, naive IL-1Ra$^{-/-}$ T cells transferred into *nu/nu* mice may be activated excessively by the endogenous physiological levels of IL-1 which are constitutively expressed in the joints (9), thereby becoming reactive against synovial components.

We showed that transplantation of IL-1Ra$^{-/-}$ BM cells induced arthritis in WT mice, and conversely, introduction of WT BM cells into IL-1Ra$^{-/-}$ mice completely suppressed the disease, indicating that BM cells and their derivatives are abnormal in IL-1Ra$^{-/-}$ mice (Figure 2). Since T cell progenitors are derived from BM cells, these observations are consistent with the notion that T cell dysfunction contributes to the development of autoimmunity. It should be noted, however, that WT mice that received IL-1Ra$^{-/-}$ BM cells took longer to develop arthritis than did nonarthritic IL-1Ra$^{-/-}$ mice that received the same BM cells. Thus, not only the donor BM cells, but also the recipient milieu, seems to be involved in the development of arthritis, suggesting that IL-1Ra from relatively radiation-resistant cells also plays a role. Since the time required for developing arthritis in WT mice that receive IL-1Ra$^{-/-}$ BM cells (3–4 months) is long enough to replace all the BM-derived cells in the recipient mice including the macrophages and type A synovial lining cells in the joint with donor type cells (16), this observation suggests that these late replacing components are involved in the development of arthritis. The observation that it took more than 16 weeks for arthritic IL-1Ra$^{-/-}$ mice that received normal BM cells to recover from the disease also supports this idea.

We have shown that the development of arthritis is completely suppressed in TNF-α$^{-/-}$ mice, indicating a crucial role for TNF-α in the pathogenesis of RA (Figure 4). In this context, a dominant role of TNF-α in the pathogenesis of RA has been demonstrated by recent clinical trials using anti-TNF-α Ab and studies in the mouse using the CIA model (3, 18, 19). It was also reported that transgenic mice carrying the *TNF-α* gene or mice deficient for the TNF-α AU-rich element (TNF$^{\Delta ARE}$), which produce higher amounts of the TNF-α protein, develop arthritis spontaneously (7, 8). However, since TNF$^{\Delta ARE}$ mice develop arthritis even in the absence of mature lymphocytes (8), cells in the innate immune system such as neutrophils, macrophages, and mast cells, rather than the T cell-dependent immune system, have been suggested to be involved in the pathogenesis of this arthritis. Likewise, it has also been reported that inflammatory cytokines such as IL-1 and TNF-α, but not IL-6, play critical roles in the effector phase of the disease in the K/BxN model, in which arthritis can be induced by serum transfer (20). The effect of TNF-α deficiency, however, was not as strong in the CIA and K/BxN models compared to that seen in the IL-1Ra$^{-/-}$ mice. Thus, the IL-1Ra$^{-/-}$ mouse is one of the most sensitive models to the effects of TNF-α.

Cell transfers showed that TNF-α$^{-/-}$ IL-1Ra$^{-/-}$ BM cells could not induce arthritis in WT recipient mice, indicating that BM-derived cells are responsible for the production of TNF-α that is crucial for the development of arthritis. Nonetheless, it is interesting that TNF-α$^{-/-}$ IL-1Ra$^{-/-}$ BM cells could induce arthritis in IL-1Ra$^{-/-}$ recipient mice but not in WT recipient mice. With regard to this, TNF-α expression is augmented in IL-1Ra$^{-/-}$ mouse joints and this TNF-α may compensate for the deficiency in BM-derived cells. It is known that T cells are sensitive to irradiation and synovial lining cells are relatively resistant to irradiation, but some of the synovial lining cells such as the type A cells are of BM origin and are eventually replaced by donor cells after BM cell transplantation. Our results suggest that TNF-α is produced by these synovial lining cells in recipient IL-1Ra$^{-/-}$ mice (Figure 3E). This TNF-α may contribute to the arthritogenic milieu observed in IL-1Ra$^{-/-}$ mice in the IL-1Ra$^{-/-}$ BM cell transfer experiments. Although some CD4$^+$ T cell populations produce TNF-α, it is unlikely that TNF-α produced by these cells is the only source of TNF-α involved in the pathogenesis because, if that were true, TNF-α$^{-/-}$ IL-1Ra$^{-/-}$ BM cells would not have induced arthritis even in IL-1Ra$^{-/-}$ recipient mice. However, since activated IL-1Ra$^{-/-}$ T cells produce high amounts of TNF-α (Table 2 and Figure 3E), it seems likely that T cell–derived TNF-α also contributes to the development of arthritis. Transfer of TNF-α$^{-/-}$ IL-1Ra$^{-/-}$ T cells into *nu/nu* mice will help evaluate this possibility, although we were not able to address this question because of the difference in the MHC locus between the TNF-α$^{-/-}$ and *nu/nu* mice.

We previously showed that IL-1 plays an important role in enhancing T cell–APC interactions by inducing CD40L and OX40 on T cells, and CD40L and OX40 expression were enhanced in T cells stimulated with antigen-bearing IL-1Ra$^{-/-}$ APCs compared to WT APCs (15). It is known that ligation of CD40 on APCs with CD40L induces OX40L expression and TNF-α production by APCs (13, 14). Here, we have shown that TNF-α induces OX40 expression on T cells (Figure 5A). Thus, the mechanism for T cell activation by IL-1 is proposed as follows. Upon interaction with antigens, APCs produce IL-1, and IL-1 activates T cells, resulting in the induction of CD40L. Then, the CD40L-CD40 interaction activates APCs to produce TNF-α. This TNF-α induces OX40 on T cells, leading to enhancement of cytokine production and activation of B cells.

IL-17 plays important roles in inflammatory diseases such as arthritis, contact hypersensitivity, asthma, and delayed-type hypersensitivity (21–23). It was recently reported that a minor subpopulation of activated CD4$^+$ T cells produces both TNF-α and IL-17 (24) and acts in synergy or additively with TNF-α and IL-1 by enhancing their production and action (25). We recently found that IL-17 production from IL-1Ra$^{-/-}$ T cells was induced by OX40 activation, and that IL-17–deficiency completely suppressed development of arthritis in IL-1Ra$^{-/-}$ mice (17). Thus, it is possible that increased OX40 expression on T cells by TNF-α may induce production of IL-17, resulting in exacerbated inflammation.

We show here that blocking CD40-CD40L and OX40-OX40L interactions inhibited the development of arthritis in IL-1Ra$^{-/-}$ mice (Figure 6). These results suggest that blocking molecules downstream of IL-1 and TNF-α in T cell activation may be effective to inhibit development of arthritis in IL-1Ra$^{-/-}$ mice. However, our results showed that once arthritis started, treatment with antibody to CD40L actually exacerbated the progression of the disease (Figure 6B). It was recently reported that activation of CD40-expressing cells has a beneficial effect on the treatment of chronic CIA (26), indicating that not only inhibition of CD40-CD40L interactions, but also CD40 ligation, can be used to reduce the autoimmune inflammatory response. Consistent with this observation, an aggressive form of polyarthritis was described in a patient with a point mutation in the *CD40L* gene (27). Thus, the CD40-CD40L system may play dual functions in the development of arthritis, and blocking the CD40-CD40L interaction by antibody treatment may also prevent beneficial effects of CD40 expression, resulting in exacerbated inflammation in IL-1Ra$^{-/-}$ mice after onset of the disease.

In summary, we have found a novel T cell regulatory mechanism in which IL-1Ra produced by T cells acts on T cells in an autocrine manner. We also showed that IL-1–induced TNF-α is crucial for the development of arthritis in IL-1Ra$^{-/-}$ mice and that this TNF-α induces OX40 on T cells. Furthermore, we showed that inhibition of either TNF-α or OX40 function is effective to suppress the development of arthritis, providing a clue for the development of new therapies for RA.

Methods

Mice. IL-1Ra$^{-/-}$ mice were produced as described (28). TNF-α$^{-/-}$ mice were kindly provided from K. Sekikawa (National Institute of Agrobiological Sciences, Tsukuba, Japan). These mice were backcrossed to the BALB/c strain mice for 8 generations. BALB/c mice, BALB/c-*nu/nu* mice, and BALB/c-*scid/scid* mice were purchased from Clea. B10.D2/n (C57BL/6 congenic) mice were purchased from Japan SLC Inc. BALB.B (BALB/c congenic) mice were provided by T. Shiroishi (National Institute of Genetics, Mishima, Japan). Age- and gender-matched mice were used in each experiment. Mice were kept under specific pathogen-free conditions in an environmentally controlled clean room at the Center for Experimental Medicine, Institute of Medical Science, University of Tokyo, Japan. The animal experiments were approved by the Committee for Animal Experiments of the Institute of Medical Science, University of Tokyo. Gene manipulation experiments were carried out according to the law for such experiments.

Thymocyte, splenocyte, and T cell preparation and transfer. Donor mice for splenocyte or arthritic T cell transfer were between 8 and 12 weeks old, and those for nonarthritic T cell transfer were between 4 and 5 weeks old. Cells were prepared from spleen, thymus, and LNs (axillary, inguinal, branchial,

cervical, and popliteal) as described previously (15). For T cell purification, spleen and LN cells were washed and passed through a nylon wool column, treated with anti-mouse B220 and Mac-1 magnetic beads and passed through a MACS column (Miltenyi Biotec). Purified $CD3^+$ T cells were less than 92% $CD3^+$. Prepared cells were resuspended in 0.2 ml PBS and i.v. transferred into BALB/*c-nu/nu* mice. Numbers of transferred cells per mouse were 10^8 cells for thymocyte transfers, 4×10^7 cells for total splenocyte transfers, and 2×10^7 cells for T cell–depleted splenocyte and T cell transfers.

Incidence of arthritis and the severity score were judged macroscopically and histologically as described previously (9). Briefly, the severity score was judged by eye: grade 0 = normal, grade 1 = light swelling of the joint and/or redness of the footpad, grade 2 = obvious swelling of the joint, and grade 3 = severe swelling and fixation of the joint. The severity score was calculated for all 4 limbs, giving a maximal score of 12 points for one mouse.

BM cell preparation and transfer. Donor mice were between 4 and 8 weeks old. BM cells from femurs, tibiae, and pelves were treated with a hemolysis buffer (17 mM Tris-HCl and 140 mM NH_4Cl, pH7.2) to remove red blood cells. T cells were removed by treating with anti-mouse Thy1.2 magnetic beads and then passed through a MACS column. T cell–depleted and purified BM cells (10^7 cells) in 0.2 ml PBS were i.v. transferred into lethally irradiated (750 rad) recipient mice.

T cell activation, cytokine ELISA, and RT-PCR. $CD4^+$ T cells were purified as described (15). Purified T cells (2×10^5 cells) were plated on a 96-well plate coated with 1 or 10 μg/ml of anti-mouse CD3 mAb (145-2C11; BD Biosciences – Pharmingen) in a final volume of 200 μl RPMI1640 plus 10% FCS and cultured for 48 hours. Culture supernatant was then collected and cell proliferation was measured by incorporation of [^{3}H] thymidine (Amersham Biosciences) (15). IFN-γ, IL-4, and TNF-α levels in culture were measured by ELISA as described previously (22, 29). For the IL-1Ra ELISA, polyclonal goat anti-mouse IL-1Ra (1 μg/ml, R&D Systems Inc.) and polyclonal biotinylated goat anti-mouse IL-1Ra (2 μg/ml, R&D Systems Inc.) Abs were used as capture and detection Abs, respectively. Streptavidin-AP (SouthernBiotech) and substrate (Sigma-Aldrich) were used for detection. Recombinant mouse IL-1Ra (R&D Systems Inc.) was used as a standard. The detection limit was 3.9 pg/ml.

Total RNAs were isolated from BALB/c T cells or T cell–depleted splenocytes using Trizol reagent (Invitrogen Corp.). RNAs were denatured in the presence of oligo (dT)12-18 primer and then reverse transcribed using SuperScript (Invitrogen) at 42°C for 1 hour. PCR was performed for 30 cycles that was within log-phase amplification stages for the PCR products. The primer sequences were as follows: IL-1Ra forward primer, 5′-GACCCTGCAAGATGCAAGCC-3′; IL-1Ra reverse primer, 5′-GAGCGGATGAAGGTAAAGCG-3′; β_2m forward primer, 5′-TGACCGGCTTGTATGCTATC-3′; β_2m reverse primer, 5′-CAGTGTGAGCCAGGATATAG-3′. These IL-1Ra primers detect both secreted and intracellular forms of IL-1Ra.

Intracellular staining of cytokines. For the intracellular staining for IL-1Ra, PECs, or $CD4^+$, T cells were prepared from BALB/c or IL-$1Ra^{-/-}$ mice. PECs were stimulated with LPS (5 μg/ml) for 3 hours, followed by LPS stimulation with 2 μM monensin for 12 hours, then cells were suspended in a staining buffer (PBS containing 2% FCS and 0.01% sodium azide). After blocking with anti-FcγRII/III receptor mAb (BD Biosciences – Pharmingen), cells were treated with FITC-anti-CD11b mAb (BD Biosciences – Pharmingen). Splenocytes were stimulated with soluble anti-CD3 mAb (1 μg/ml), and purified $CD4^+$ T cells were stimulated with plate-coated anti-CD3 mAb (1 μg/ml) for 72 hours, and the GolgiPlug (BD Biosciences – Pharmingen) was added for the final 6 hours of stimulation. Cells were treated with anti-FcγRII/III receptor mAb and stained with cychrome-anti-CD4 mAb (BD Biosciences – Pharmingen). These cells were then fixed with PBS containing 4% paraformaldehyde for 20 minutes. After washing with a permeabilization buffer (PBS containing 10 mM HEPES, 0.1% BSA, and 0.5% Triton X-100), cells were incubated with goat anti-mouse IL-1Ra Ab (R&D Systems Inc.) or isotype-matched control Ab (goat IgG; R&D Systems Inc.) in the permeabilization buffer for 30 minutes at 4°C. Cells were then washed with the permeabilization buffer and stained with Cy5-donkey-anti-goat IgG (Jackson ImmunoResearch Laboratories).

For intracellular cytokine staining for IFN-γ, IL-4, and TNF-α, synovial tissues were dissected from the ankle joints of IL-$1Ra^{-/-}$ mice who had already developed arthritis and normal ankle joints of WT mice. These joints were digested in a cocktail of 2.4 mg/ml hyaluronidase (Sigma-Aldrich), 1 mg/ml collagenase (Wako Pure Chemical Industries) and 100 μg/ml DNase I (Sigma-Aldrich) in RPMI plus 10% FBS for 1.5 hours at 37°C. The cells were filtered through a nylon mesh, washed with RPMI plus 10% FBS, then stimulated with PMA (10 ng/ml) and Ionomycin (400 ng/ml; Sigma-Aldrich) for 6 hours at 37°C with 2 μM monensin. These cells were blocked with anti-FcγRII/III receptor mAb and stained with cell lineage–specific Abs against cell surface molecules, then fixed in 4% paraformaldehyde for 20 minutes, resuspended in the permeabilization buffer, and stained with anti-cytokine Abs for 45 minutes at 4°C. Abs used for the cell lineage-specific staining were as follows: FITC-anti-CD11b, allophycocyanin-anti-TCR-β, CyChrome-anti-CD4, and allophycocyanin-anti-CD8 (BD Biosciences – Pharmingen). Those used for intracellular staining were as follows: PE-anti-IFN-γ, PE-anti-IL-4 (BD Biosciences – Pharmingen), and PE-anti-TNF-α (eBioscience). Cells were washed with the permeabilization buffer and analyzed using FACSCalibur by CellQuest software (BD).

Flow cytometric analysis of costimulatory molecules. CD40L and OX40 expression on $CD4^+$ T cells was analyzed as described previously (15). Briefly, for CD40L expression, purified $CD4^+$ T cells on 12-well plates (1×10^6 cells/well) were stimulated with plate-coated anti-CD3 mAb with or without mouse recombinant TNF-α (Peprotech) in the presence of 1 μg of biotinylated anti-mouse CD40L mAb (MR-1; BD Biosciences – Pharmingen) or biotinylated hamster IgG (eBioscience) as an isotype-matched control Ab for 24 hours. For OX40 expression, $CD4^+$ T cells were stimulated with plate-coated anti-CD3 mAb with or without TNF-α for 72 hours. Cells were stained with allophycocyanin-anti-mouse-CD4 mAb (PharMingen) and either biotinylated anti-mouse OX40 mAb (OX86, eBioscience) or biotinylated rat IgG (eBioscience), followed by staining with PE-streptavidin (BD Biosciences – Pharmingen).

Antibody preparation and treatment. Anti-OX40L Ab and anti-CD40L Ab were produced in hybridoma cell lines, MGP34 and MR-1, respectively. For OX40L Ab preparation, hybridoma cells were allowed to proliferate in ascites of *nu/nu* mice for 7–10 days or cultured in serum-free medium with the iMAb Monoclonal Antibody Production Kit (Diagnostic Chemicals Ltd.) for 4 weeks. Ascites and culture supernatant was collected and Abs were purified using Protein A column (Amersham Biosciences). For CD40L Ab preparation, hybridoma cells were cultured in serum-free medium for 4 weeks. Supernatant was collected and Abs were purified using Protein G column (Amersham Biosciences). Anti-OX40L Ab (500 μg) or anti-CD40L Ab (250 μg) was intraperitoneally injected into nonarthritic IL-$1Ra^{-/-}$ mice twice a week for 6 weeks. Rat IgG or hamster IgG (Cappel, ICN Pharmaceuticals) was injected as the isotype control for anti-OX40L or anti-CD40L Ab, respectively. Mice treated with Abs were between 4 and 6 weeks old. Arthritic score was inspected at the time of Ab injection.

Statistics. The repeated-measures ANOVA–Fisher's protected least significant different test (post hoc test) or the chi-square test for independence was used for statistical evaluation of incidence. The 2-way ANOVA was used for statistical evaluation of the arthritic score. The statistical significance of affected mice scores was calculated from the point at which 2 or more mice of each genotype became arthritic. The Student's *t* test was used for statistical evaluation of the results except for incidence and score.

Acknowledgments

We thank K. Sekikawa for TNF-$\alpha^{-/-}$ mice, T. Shiroishi for BALB.B mice, S. Mori and T. Nakajima (University of Tokyo, Tokyo, Japan) for histological sections, and S.J. Galli (Stanford University School of Medicine, Stanford, California, USA) for support in the experiments. We also thank all the members of the lab for their discussion and help in animal care. This work was supported by grants from the Ministry of Education, Culture, Sport, and Science of Japan; the Ministry of Health and Welfare of Japan; CREST; the Japan Society for the Promotion of Science; and the Japan Rheumatism Foundation.

Received for publication December 5, 2003, and accepted in revised form October 5, 2004.

Address correspondence to: Yoichiro Iwakura, Center for Experimental Medicine, Institute of Medical Science, University of Tokyo, Shirokanedai, Minato-ku, Tokyo 108-8639, Japan. Phone: 81-3-5449-5536, Fax: 81-3-5449-5430; E-mail: iwakura@ims.u-tokyo.ac.jp.

Susumu Nakae's present address is: Department of Pathology, Stanford University School of Medicine, Stanford, California, USA.

Taizo Matsuki's present address is: Japan Science and Technology Agency, Tokyo, Japan.

Katsuko Sudo's present address is: Animal Research Center, Tokyo Medical University, Tokyo, Japan.

1. Feldmann, M., Brennan, F.M., and Maini, R.N. 1996. Role of cytokines in rheumatoid arthritis. *Annu. Rev. Immunol.* **14**:397–440.
2. Firestein, G.S., and Zvaifler, N.J. 1992. Rheumatoid arthritis: a disease of disordered immunity. In *Inflammation: basic principles and clinical correlates.* 2nd edition. J.I. Gallin, I.M. Goldstein, and R. Snyderman, editors. Raven Press, Ltd. New York, New York, USA. 959–975.
3. Feldmann, M., and Maini, R.N. 2001. Anti-TNF-α therapy of rheumatoid arthritis: what have we learned? *Annu. Rev. Immunol.* **19**:163–196.
4. Tocci, M.J., and Schmidt, J.A. 1997. Interleukin-1: Structure and function. In *Cytokines in health and disease.* 2nd edition. D.G. Remick and J.S. Friedland, editors. Marcel Dekker, Inc. New York, New York, USA. 1–27.
5. Iwakura, Y. 2002. Roles of IL-1 in the development of rheumatoid arthritis: consideration from mouse models. *Cytokine Growth Factor Rev.* **13**:341–355.
6. Arend, W.P., Malyak, M., Guthridge, C.J., and Gabay, C. 1998. Interleukin-1 receptor antagonist: role in biology. *Annu. Rev. Immunol.* **16**:27–55.
7. Kollias, G., Douni, E., Kassiotis, G., and Kontoyiannis, D. 1999. On the role of tumor necrosis factor and receptors in models of multiorgan failure, rheumatoid arthritis, multiple sclerosis and inflammatory bowel disease. *Immunol. Rev.* **169**:175–194.
8. Kontoyiannis, D., Pasparakis, M., Pizarro, T.T., Cominelli, F., and Kollias, G. 1999. Impaired on/off regulation of TNF biosynthesis in mice lacking TNF AU-rich elements: implications for joint and gut-associated immunopathologies. *Immunity.* **10**:387–398.
9. Horai, R., et al. 2000. Development of chronic inflammatory arthropathy resembling rheumatoid arthritis in interleukin 1 receptor antagonist-deficient mice. *J. Exp. Med.* **191**:313–320.
10. Niki, Y., et al. 2001. Macrophage- and neutrophil-dominant arthritis in human IL-1α transgenic mice. *J. Clin. Invest.* **107**:1127–1135.
11. Mima, T., et al. 1995. Transfer of rheumatoid arthritis into severe combined immunodeficient mice. The pathogenetic implications of T cell populations oligoclonally expanding in the rheumatoid joints. *J. Clin. Invest.* **96**:1746–1758.
12. Weinberg, A.D. 1998. Antibodies to OX-40 (CD134) can identify and eliminate autoreactive T cells: implications for human autoimmune disease. *Mol. Med. Today.* **4**:76–83.
13. van Kooten, C., and Banchereau, J. 2000. CD40-CD40 ligand. *J. Leukoc. Biol.* **67**:2–17.
14. Weinberg, A.D. 2002. OX40: targeted immunotherapy – implications for tempering autoimmunity and enhancing vaccines. *Trends Immunol.* **23**:102–109.
15. Nakae, S., Asano, M., Horai, R., Sakaguchi, N., and Iwakura, Y. 2001. IL-1 enhances T cell-dependent antibody production through induction of CD40 ligand and OX40 on T cells. *J. Immunol.* **167**:90–97.
16. Kitagawa, H., et al. 1993. Analyses of origin of synovial cells and repairing mechanisms of arthritis by allogeneic bone marrow transplantation. *Immunobiology.* **188**:99–112.
17. Nakae, S., et al. 2003. IL-17 production from activated T cells is required for the spontaneous development of destructive arthritis in mice deficient in IL-1 receptor antagonist. *Proc. Natl. Acad. Sci. U. S. A.* **100**:5986–5990.
18. Thorbecke, G.J., et al. 1992. Involvement of endogenous tumor necrosis factor α and transforming growth factor β during induction of collagen type II arthritis in mice. *Proc. Natl. Acad. Sci. U. S. A.* **89**:7375–7379.
19. Joosten, L.A., et al. 1999. IL-1αβ blockade prevents cartilage and bone destruction in murine type II collagen-induced arthritis, whereas TNF-α blockade only ameliorates joint inflammation. *J. Immunol.* **163**:5049–5055.
20. Ji, H., et al. 2002. Critical roles for interleukin 1 and tumor necrosis factor α in antibody-induced arthritis. *J. Exp. Med.* **196**:77–85.
21. Lubberts, E., et al. 2001. IL-1-independent role of IL-17 in synovial inflammation and joint destruction during collagen-induced arthritis. *J. Immunol.* **167**:1004–1013.
22. Nakae, S., et al. 2002. Antigen-specific T cell sensitization is impaired in IL-17-deficient mice, causing suppression of allergic cellular and humoral responses. *Immunity.* **17**:375–387.
23. Nakae, S., Nambu, A., Sudo, K., and Iwakura, Y. 2003. Suppression of immune induction of collagen-induced arthritis in IL-17-deficient mice. *J. Immunol.* **171**:6173–6177.
24. Infante-Duarte, C., Horton, H.F., Byrne, M.C., and Kamradt, T. 2000. Microbial lipopeptides induce the production of IL-17 in Th cells. *J. Immunol.* **165**:6107–6115.
25. Chabaud, M., and Miossec, P. 2001. The combination of tumor necrosis factor alpha blockade with interleukin-1 and interleukin-17 blockade is more effective for controlling synovial inflammation and bone resorption in an ex vivo model. *Arthritis Rheum.* **44**:1293–1303.
26. Mauri, C., Mars, L.T., and Londei, M. 2000. Therapeutic activity of agonistic monoclonal antibodies against CD40 in a chronic autoimmune inflammatory process. *Nat. Med.* **6**:673–679.
27. Webster, E.A., et al. 1999. An aggressive form of polyarticular arthritis in a man with CD154 mutation (X-linked hyper-IgM syndrome). *Arthritis Rheum.* **42**:1291–1296.
28. Horai, R., et al. 1998. Production of mice deficient in genes for interleukin (IL)-1α, IL-1β, IL-1α/β, and IL-1 receptor antagonist shows that IL-1β is crucial in turpentine-induced fever development and glucocorticoid secretion. *J. Exp. Med.* **187**:1463–1475.
29. Nakae, S., Asano, M., Horai, R., and Iwakura, Y. 2001. Interleukin-1β, but not interleukin-1α, is required for T-cell-dependent antibody production. *Immunology.* **104**:402–409.

Synapse. 2003 Jan;47(1):54-7.

Interleukin-1beta abrogates long-term depression of hippocampal CA1 synaptic transmission.

Ikegaya Y, Delcroix I, Iwakura Y, Matsuki N, Nishiyama N.

Laboratory of Chemical Pharmacology, Graduate School of Pharmaceutical Sciences, The University of Tokyo, Tokyo 113-0033, Japan. ikegaya@tk.airnet.ne.jp

Although interleukin-1beta (IL-1beta) is well known to modulate synaptic transmission and plasticity of the hippocampus, no study has yet evaluated how this cytokine affects long-term depression (LTD), one of the major forms of hippocampal synaptic plasticity. Here we report that at Schaffer collateral-CA1 synapses, bath application of IL-1beta induces a long-lasting decrease in synaptic strength in intact slices, but not in disinhibited slices in the presence of bicuculline, a gamma-aminobutyric acid receptor antagonist. The IL-1beta-induced synaptic depression efficiently foreclosed the subsequent induction of LTD in response to a 1-Hz tetanus and, conversely, it was also prevented by preexisting LTD. These results suggest that IL-1beta-induced, persistent depression of synaptic efficacy is required for GABAergic activation and shares, at least in part, a common cellular mechanism for LTD.

MOLECULAR AND CELLULAR BIOLOGY, Jan. 2003, p. 55–61 Vol. 23, No. 1
0270-7306/03/$08.00+0 DOI: 10.1128/MCB.23.1.55–61.2003

Phenotypic Analysis of Meltrin α (ADAM12)-Deficient Mice: Involvement of Meltrin α in Adipogenesis and Myogenesis

Tomohiro Kurisaki,[1] Aki Masuda,[1] Katsuko Sudo,[2] Junko Sakagami,[2] Shigeki Higashiyama,[3] Yoichi Matsuda,[4,5] Akira Nagabukuro,[5] Atsushi Tsuji,[5] Yoichi Nabeshima,[6] Masahide Asano,[7] Yoichiro Iwakura,[2] and Atsuko Sehara-Fujisawa[1]*

Field of Growth Regulation, Institute for Frontier Medical Sciences, Kyoto University, Kyoto 606-8507,[1] Center for Experimental Medicine, Institute of Medical Science, University of Tokyo, Tokyo 108-8639,[2] Department of Medical Biochemistry, Ehime University School of Medicine, Ehime 791-0295,[3] Laboratory of Animal Cytogenetics, Center for Advanced Science and Technology, Hokkaido University, Sapporo 060-0810,[4] Laboratory of Animal Genetics, Graduate School of Bioagricultural Science, Nagoya University, Chikusa-ku, Nagoya 464-8601,[5] Department of Pathology and Tumor Biology, Kyoto University Graduate School of Medicine, Kyoto 606-8501,[6] and Institute for Experimental Animals, School of Medicine, Kanazawa University, Kanazawa 920-8640,[7] Japan

Received 29 May 2002/Returned for modification 28 August 2002/Accepted 7 October 2002

Meltrin α (ADAM12) is a metalloprotease-disintegrin whose specific expression patterns during development suggest that it is involved in myogenesis and the development of other organs. To determine the roles Meltrin α plays in vivo, we generated Meltrin α-deficient mice by gene targeting. Although the number of homozygous embryos are close to the expected Mendelian ratio at embryonic days 17 to 18, ca. 30% of the null pups born die before weaning, mostly within 1 week of birth. The viable homozygous mutants appear normal and are fertile. Most of the muscles in the homozygous mutants appear normal, and regeneration in experimentally damaged skeletal muscle is unimpeded. In some Meltrin α-deficient pups, the interscapular brown adipose tissue is reduced, although the penetrance of this phenotype is low. Impaired formation of the neck and interscapular muscles is also seen in some homozygotes. These observations suggest Meltrin α may be involved in regulating adipogenesis and myogenesis through a linked developmental pathway. Heparin-binding epidermal growth factor-like growth factor (HB-EGF) is a candidate substrate of Meltrin α, and we found that TPA (12-*O*-tetradecanoylphorbol-13-acetate)-induced ectodomain shedding of HB-EGF is markedly reduced in embryonic fibroblasts prepared from Meltrin α-deficient mice. We also report here the chromosomal locations of Meltrin α in the mouse and rat.

Meltrin α is a metalloprotease-disintegrin that belongs to the ADAM (for "a disintegrin and metalloprotease") family. To date, more than 30 ADAMs in worms, flies, rodents, primates, and humans have been identified (3, 44). ADAMs are thought to be involved in various biological functions, including fertilization, myogenesis, neurogenesis, and the development of various epithelial tissues (3, 30, 35). For example, Fertilin α and Fertilin β, which were the first identified mammalian ADAMs, play important roles in fertilization (4, 8). Another example is Kuzbanian (ADAM10), which is known to be involved in neurogenesis by regulating Notch signaling (18, 28, 31, 40). Some ADAMs are catalytically active metalloproteases and participate in the proteolytic processing of the extracellular domains of membrane-anchored proteins (44). For example, TACE (ADAM17) was initially identified as the protease responsible for the processing of tumor necrosis factor alpha (2, 23). Studies on TACE-null mice then revealed that TACE is involved in the processing of the extracellular domains of several membrane-anchored proteins, including the tumor necrosis factor p75 receptor, the adhesion molecule L-selectin, the amyloid precursor protein, and transforming growth factor α (7). Another example is Meltrin β (ADAM19), which has been shown to be involved in the in vitro processing of Neuregulin β, another membrane-anchored growth factor (37). Other studies suggest that ADAMs are also involved in cell-cell or cell-extracellular matrix interactions through their interaction with integrins (6, 10, 27, 48) or proteoglycans (15).

We previously showed that Meltrin α promotes myotube formation in vitro (45). Furthermore, Meltrin α is specifically expressed in the muscles during the neonatal stages and in the bones of both neonates and adults. In addition, during embryogenesis, Meltrin α mRNA was found in the mesenchymes of the lungs and the intestines and in the placenta (17), which suggests that Meltrin α is involved in organogenesis. Based on its amino acid sequence, the metalloprotease domain of Meltrin α is presumed to be catalytically active. Supporting this notion are the reports that it has proteolytic activity in vitro. For example, human Meltrin α interacts with insulin-like growth factor-binding protein 3 (IGFBP-3) (36) and cleaves it in vitro (19). Furthermore, Meltrin α has also recently been implicated to act as a sheddase with heparin-binding epidermal growth factor-like growth factor (HB-EGF) (1). To further determine the function of Meltrin α in mouse development, we generated and analyzed Meltrin α gene-targeted mice.

* Corresponding author. Mailing address: Field of Growth Regulation, Institute for Frontier Medical Sciences, Kyoto University, Kyoto, 606-8507, Japan. Phone: 81-75-751-3826. Fax: 81-75-751-4642. E-mail: asehara@frontier.kyoto-u.ac.jp.

Materials and Methods

Materials. Chemicals were purchased from Sigma (St. Louis, Mo.) and nacalai tesque (Kyoto, Japan). Restriction enzymes and reagents for molecular biology were purchased from TaKaRa (Kyoto, Japan) and Toyobo (Osaka, Japan) unless otherwise indicated.

Construction of Meltrin α gene-targeting vector. The Meltrin α gene isolated from a 129/SvJ genomic library (Stratagene) was used to construct the targeting vector. The PGKneobpA cassette from pPGKneobpA (39) was inserted between a 5′ homologous region (*Xho*I-*Bam*HI [9 kb]) and a 3′ homologous region (*Sac*II-*Sac*I [1.5 kb]). The DT-A cassette (46) was ligated at the 3′ end of the targeting vector for negative selection. In this construct, the exon containing the initiation codon was deleted.

Generation of Meltrin $\alpha^{-/-}$ mice. The linearized targeting vector (20 μg) was electroporated (250 V, 500 μF) into 10^7 R1 embryonic stem (ES) cells (26) and selected with 180 μg (active form) of G418 (Gibco-BRL)/ml for 7 to 10 days. Homologous recombinants were selected by PCR and confirmed by Southern blot analysis. The forward primer in the PGKneobpA cassette was 5′-TGGAT GTGGAATGTGTGCGAGG-3′, and the reverse primer outside the targeting vector was 5′-TTCCATTGCTCAGCGGTGCTGTC-3′. PCR was performed with LA *Taq* DNA polymerase (TaKaRa, Kyoto, Japan) for 30 cycles at 98°C for 20 s and at 68°C for 10 min in a volume of 50 μl. Two ES clones that yielded hybridization bands of the correct size gave rise to germ line chimeras by the aggregation method (26). The resulting chimeras were backcrossed to C57BL/6J, and N_8 mice were used in the following experiments. The genotypes were determined by either PCR (for embryos) or Southern blot analysis. Genotyping PCR was performed as follows: the primer set in the PGKneobpA cassette (5′-TGGAGAGGCTATTCGGCTATGACTGGG-3′ and 5′-ATGCAGCCGCC GCATTGCAT-3′) was used to detect targeted alleles. PCR was performed with Ampli*Taq* Gold DNA polymerase (PE Applied Biosystems) for 40 cycles at 96°C for 15 s and at 70°C for 30 s in a volume of 15 μl. The primer set in the exon containing the initiation codon (5′-GCGCTCTGCCATTGTCGCCG-3′ and 5′-GGCAGACTCAGGGCAGTAGGACTTCCC-3′) was used to detect wild-type alleles. PCR conditions used were the same as those for the targeted allele detection PCR, except that the annealing and extension temperatures used were both 64°C. Southern blot and reverse transcription-PCR (RT-PCR) analyses were performed as follows: genomic DNA from ES cells or mouse tail was digested with restriction enzymes, electrophoresed through a 0.8% agarose gel and transferred to Hybond-XL membrane (Amersham Pharmacia Biotech). Hybridization was performed according to standard methods (33) with a ^{32}P-labeled DNA probe made by using a Megaprime DNA labeling kit (Amersham Pharmacia Biotech). A 1.2-kb *Sac*I-*Hin*dIII fragment immediately downstream of the 3′ end of the 3′ homology region was used as the probe. RT-PCR was performed as follows. mRNA was extracted from embryos by using a QuickPrep Micro mRNA purification kit (Amersham Pharmacia Biotech). cDNA was synthesized from the mRNA by using the SuperScript first-strand synthesis system (Invitrogen). PCR was carried out with Ampli*Taq* Gold DNA polymerase. The primers used to detect mRNA of Meltrin α were 5′-GATGACCAAGTACGTAGAGC TGG-3′ and 5′-TCATGGAGCCTGGTGAATGGG-3′ (for the metalloprotease domain), 5′-GAGTGTGACTGCGGAGAACCGGAGGAA-3′ and 5′-ATTTT CCCACACTTGGCATCTCTCA-3′ (for the disintegrin domain), 5′-GTCAAG GTGGTGCAAGCCGA-3′ and 5′-TGATGGGACCACTGTCTGTGC-3′ (for the cysteine-rich domain), and 5′-GACGTTGATGCGGCTGCTGTTC-3′ and 5′-GCGTCGAGGGGCCTGCTGATG-3′ (for the cytoplasmic domain). The glyceradehyde-3-phosphate dehydrogenase 0.45-kb control amplimer set (Clontech) was used as a positive control. Mice were maintained under specific-pathogen-free conditions in environmentally controlled clean rooms at the Laboratory Animal Research Center, Institute of Medical Science, University of Tokyo, the Animal Facility, Tokyo Institute of Medical Science, and at the Institute for Frontier Medical Sciences, Kyoto University. The experiments were conducted according to institutional ethical guidelines for animal experimentation and safety guidelines for gene manipulation experiments.

Histology. Embryos were fixed in 4% paraformaldehyde–phosphate-buffered saline (PBS). Fixed samples were dehydrated by sequentially increased ethanol concentrations, cleared in xylene, and then embedded in paraffin. The embedded samples were sectioned into 4.5-μm-thick slices and stained with hematoxylin and eosin (HE).

In situ hybridization. In situ hybridization was performed with digoxigenin-labeled antisense and sense riboprobes prepared by in vitro transcription according to the manufacturer's protocol (Roche Molecular Biochemicals). The antisense probe for Meltrin α consisted of two 1.3-kb fragments that spanned nucleotides 93 to 1417 and nucleotides 1997 to 3338.

Mouse embryonic fibroblasts. Embryonic day 13.5 (E13.5) embryos from Meltrin α knockout and wild-type mice were used to generate mouse embryonic fibroblasts (14). Briefly, the head, limbs, and viscera were removed from the embryos, and the carcasses were minced and then trypsinized in 0.05% trypsin 0.02% EDTA in PBS for 10 min at 37°C. Cells were collected and grown in 10% fetal calf serum in Dulbecco's modified Eagle medium (DMEM).

HB-EGF ectodomain shedding assay. Embryonic fibroblast cells prepared from wild-type and knockout mice were seeded in 6-cm dishes at a density of 2×10^5 cells/dish and cultured for 48 h with DMEM–10% fetal calf serum. Cells were incubated for 1 h at 37°C with 100 nM TPA (12-*O*-tetradecanoylphorbol-13-acetate). Cells were washed three times with ice-cold Hanks buffer and biotinylated with 0.1 mg of sulfo-NHS-biotin/ml in 50 mM HEPES (pH 7.5)–0.15 M NaCl for 10 min on ice. Excess reagent was quenched and removed by washing with ice-cold DMEM-fetal calf serum. Cells were lysed with a buffer containing 1% Triton X-100, 1 mM EDTA, 1 mM (*p*-amidinophenyl)methanesulfonyl fluoride HCl, 1 μg of aprotinin/ml, and 0.4 M NaCl in 20 mM HEPES (pH 7.2). After centrifugation of the lysates at 15,000 rpm for 10 min, supernatants were collected and incubated with 2 μg of HB-EGF antibody H1 for 2 h at 4°C, followed by incubation with 10 μl of protein G-Sepharose (50% suspension) for 2 h at 4°C. After centrifugation of the mixes, the pellets were analyzed by sodium dodecyl sulfate-polyacrylamide gel electrophoresis and Western blotting as described previously (13).

FISH. The chromosomal assignment of the murine and rat Meltrin α genes was made by direct R-banding fluorescence in situ hybridization (FISH) with a mouse cDNA fragment as a probe (nucleotides 93 to 1417). Chromosome preparation and FISH detection were performed as described previously (21, 22).

RESULTS

Generation of Meltrin α-deficient mice. Meltrin α-deficient mice were generated by homologous recombination. The exon containing the initiation codon was replaced with the neomycin-resistant cassette (Fig. 1a). Homologous recombination was confirmed by Southern blot analysis (Fig. 1b). The hetero- and homozygotes had a normal appearance, and the males and females were both fertile. To confirm that homozygotes do not express Meltrin α, RT-PCR was performed. PCR primer sets for each of the metalloprotease, disintegrin, cysteine-rich, and cytoplasmic domains of Meltrin α did not detect Meltrin α mRNA in the homozygous mutant embryos (E14.5) (Fig. 1c). Despite the normal appearance of the null homozygotes, the number of these homozygotes at weaning was lower than the expected Mendelian ratio in the heterozygous crosses, although the ratio of wild types, heterozygotes, and homozygotes was Mendelian prior to birth (E16.5 to E18.5) (Table 1). That is, during the perinatal period, especially P1-2, the number of homozygous mutants declined, with ca. 30% of the homozygotes dying before weaning. The cause of death is still unclear. Similar results were observed for both of our lines of Meltrin α-deficient mice, which were obtained from independent ES clones.

Histological analysis of Meltrin $\alpha^{-/-}$ embryos. The Meltrin α-deficient mice appeared grossly normal at weaning. However, detailed anatomical analysis of neonatal mice revealed that the interscapular brown adipose tissue (BAT) was reduced in ca. 30% of the Meltrin α-deficient mice (Fig. 2). Although the number and morphology of the adipose lobes were similar to those of wild-type mice, the lobes were significantly smaller. Some of the homozygotes exhibited looser condensation of adipocytes than the wild-type or heterozygous littermates at ca. E16.5, probably due to the lower cell number (data not shown). In addition, some of the perinatal and newborn homozygotes (E17.5-P1) showed impaired formation of the neck and interscapular muscles (Fig. 2f). Although these muscles occupy

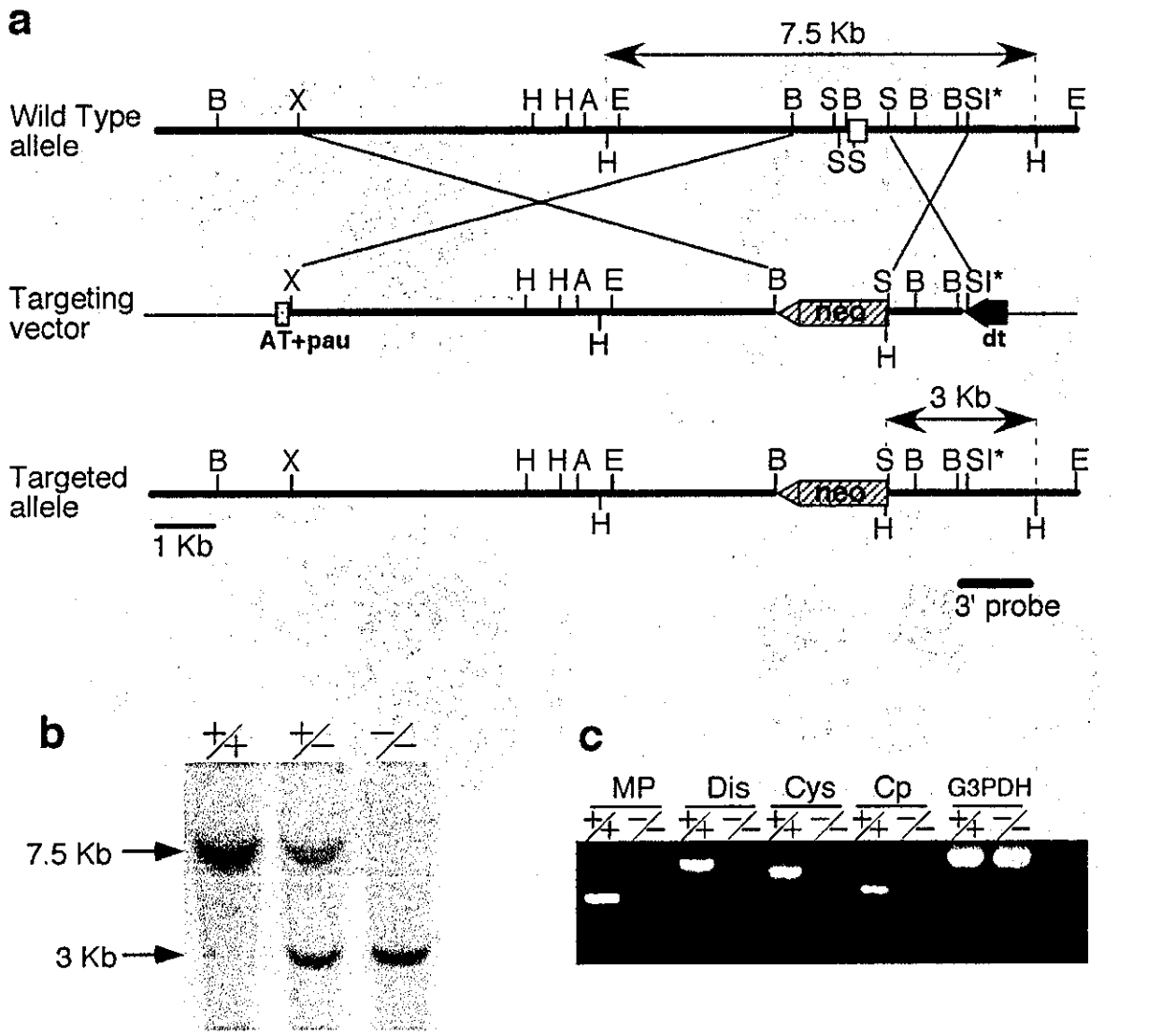

FIG. 1. Generation of Meltrin α-deficient mice. (a) Targeted disruption of the Meltrin α gene. Exon 1 containing the first methionine codon (open box) was replaced by a neocassette. Neo (hatched box) is the neomycin resistance gene, AT+pau (dotted box) indicates the AT-rich RNA polymerase II destabilizing signal and pausing signal, and DT (closed box) is the diphtheria toxin A fragment cassette. The 3′ probe represents the position of the external probe used for Southern blot analysis, and the expected *Hin*dIII fragments are indicated by arrows. Abbreviations: B, *Bam*HI; X, *Xho*I; H, *Hin*dIII; A, *Asp*718; E, *Eco*RI; S, *Sac*II; SI, *Sac*I. The asterisk indicates that the *Sac*I sites in the targeting vector are not unique. (b) Southern blot analysis of mouse tail genomic DNA. The expected DNA fragments for the targeted allele and the wild-type allele are 3 and 7 kb, respectively. +/+, wild-type; +/−, heterozygote; −/−, homozygote. (c) RT-PCR analysis of mRNA from embryonic fibroblasts isolated from E13.5 embryos. MP, primer detecting the metalloprotease domain; Dis, primer detecting the disintegrin domain; Cys, primer detecting the cysteine-rich domain; Cp, primer detecting the cytoplasmic domain. +/−, heterozygote; −/−, homozygote.

areas between the bone and skin that are similar in size to that in the wild type or heterozygotes, the muscle fibers close to the adipose tissues were found not to be as tightly packed in some homozygotes as in the non-null littermates. Although the number of homozygous neonates with impaired BAT or interscapular muscle formation was low (ca. 30%), such defects were never observed in wild-type neonates. However, at 8 weeks of age, all homozygous mice had normal-sized BATs, although some of the interscapular muscles remained slightly reduced in size (data not shown). Since it was not possible to monitor individual mice throughout development, it is not clear

TABLE 1. Genotypic analysis of mice from intercrosses[a]

Mating (female vs male)	Age	No. (%) of mice with genotype:		
		+/+	+/−	−/−
+/− vs +/−	3 wk	66 (30.8)	101 (47.2)	47 (22.0)
	P1-P2	51 (29.0)	92 (52.3)	33 (18.8)
	E16.5-E18.5	25 (23.6)	46 (43.4)	35 (33.0)
+/− vs −/−	3 wk		80 (58.4)	57 (41.6)[b]

[a] +/+, wild type; +/−, heterozygote; −/−, homozygote.
[b] $P < 0.03$.

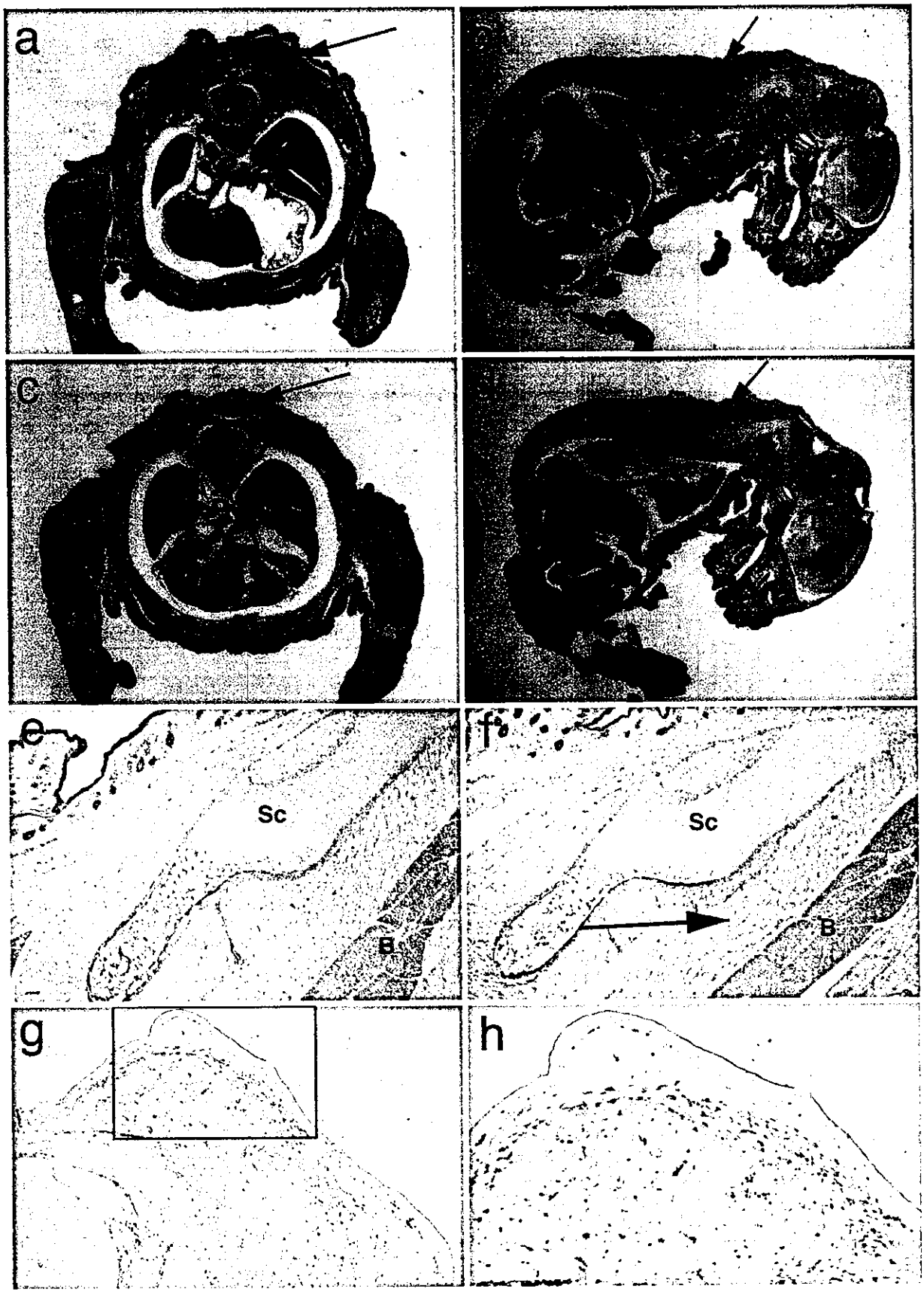
a
c
e
Sc
B
f
Sc
B
g
h

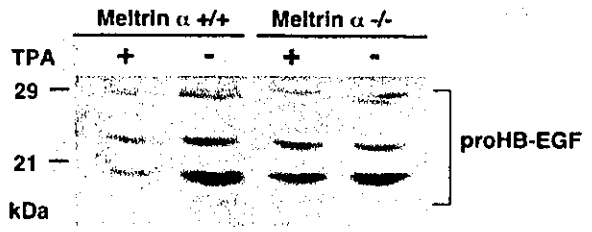

FIG. 3. HB-EGF ectodomain shedding assay. Detection of surface proHB-EGF in mouse embryonic fibroblasts treated with or without TPA. The multiple bands of proHB-EGF are derived from various N-terminal truncations and heterogeneous glycosylations.

whether the size of the BAT recovers after birth or whether mutants with small BATs die.

Muscle regeneration in Meltrin-α-deficient mice. Meltrin-α is activated both in vitro and in vivo during the differentiation of muscle satellite cells (5). Thus, we evaluated the effect Meltrin-α deficiency has on muscle regeneration. When the anterior tibial muscles of adult Meltrin α-deficient mice were experimentally damaged by cardiotoxin treatment, muscle regeneration comparable to that of wild-type mice was observed (data not shown). When we crossed Meltrin α-deficient mice with *mdx* mice, which are muscular dystrophy mutants that show enhanced muscle degeneration and muscle regeneration (9, 41), no enhancement of muscle degeneration or decreased regeneration was observed in the Meltrin-α *mdx* double mutants (data not shown).

Expression of Meltrin α in the BAT-forming region during embryogenesis. In situ hybridization was performed to analyze the expression pattern of Meltrin α during BAT development in the heterozygotes. At E14.5, Meltrin α transcripts were detected in mesenchymal cells in the BAT-forming region beneath the skin (Fig. 2g and h). These Meltrin-α-expressing mesenchymal cells extended to the region of the developing neck muscles adjacent to the BAT tissues, suggesting that these Meltrin α-positive mesenchymal cells are involved in the embryonic development of BAT and adjacent muscle tissues.

HB-EGF ectodomain shedding. Recent studies with metalloprotease inhibitors have implicated metalloproteases in the ectodomain shedding of HB-EGF (1). Therefore, we examined whether Meltrin α can act as a sheddase of HB-EGF in mouse embryonic fibroblasts prepared from E13.5 Meltrin α-deficient or wild-type embryos. Expression of Meltrin α in embryonic fibroblasts was confirmed by RT-PCR (Fig. 1c). Endogenous HB-EGF was detected by cell surface biotinylation, immunoprecipitation, and Western blotting. HB-EGF shedding was evaluated in untreated cells and in TPA-treated cells (Fig. 3). In wild-type embryonic fibroblasts, TPA induced the processing of proHB-EGF (the membrane-anchored form), resulting in the loss of the cell surface proHB-EGF. In contrast, TPA did not induce processing of proHB-EGF in Meltrin α-deficient embryonic fibroblasts. This suggests that Meltrin α contributes to the ectodomain shedding of HB-EGF.

Chromosomal mapping of the murine and rat meltrin α genes. The chromosomal locations of the murine and rat meltrin α genes were determined by direct R-banding FISH with a murine cDNA fragment as a probe (Fig. 4). The Meltrin α genes were localized to the F3 distal −F4 band of mouse chromosome 7 and the q43 proximal band of rat chromosome 1. Conserved linkage homology between these species has been identified in these areas (20, 21, 34, 38, 47). To date, suggestive mutations have not been mapped to Meltrin α. We attempted to linkage map the Meltrin α gene by interspecific backcross analysis with progeny derived from the mating of (C57BL6 3 *Mus spretus*)F_1 × *M. spretus* mice. However, this attempt failed because of the presence of an additional Meltrin α-like gene in *M. spretus* chromosome 2.

DISCUSSION

Meltrin α (ADAM12) was originally cloned from myogenic cells. Its expression pattern suggests that it is involved in various organogenic processes, particularly myogenesis (12, 17, 45). In the present study, we examined the function of Meltrin α during mouse development by generating mice lacking the Meltrin α gene. Unexpectedly, no major morphological abnormalities were observed in Meltrin $\alpha^{-/-}$ mice, and the homozygous mutants were viable and fertile. However, ca. 30% of homozygotes did die within 1 week of birth. The cause of death is unknown. In addition, some homozygous mutants showed impaired formation of interscapular BAT (E17.5-P1).

Mammals have two types of adipose tissue, namely, white adipose tissue (WAT) and BAT (32). Although WAT stores excess energy as triglycerides and releases free fatty acids in response to energy requirements, BAT dissipates energy in the form of heat through the uncoupling of oxidative phosphorylation. It functions as a thermogenerator to maintain the body temperature and protects against obesity. Thus, the impaired formation of BAT can cause hypothermia in neonates. Parents sometimes do not nurse neonates with low body temperatures, which might explain the semilethality of the homozygous mutant neonates. Nevertheless, all surviving adult homozygous mutants had apparently normal BAT and WAT (perigonadal).

It is noteworthy that some Meltrin α-deficient mice also show hypotrophy of muscles adjacent to BAT and that others show a reduction of both tissues. In vitro studies have revealed that both muscle and fat cells can be induced from pluripotent stem cell lines or marrow-derived stromal cells (29, 42). Although the identity and mechanisms of differentiation of such presumptive mesenchymal precursor cells remains unknown, the embryonic expression of Meltrin α and the effect of its absence on BAT and adjacent muscle formation shown in the present study support the idea that the development of these tissues are intimately related. Furthermore, recent studies

FIG. 2. Histological analysis of Meltrin $\alpha^{-/-}$ embryos. Heterozygous (a, b, and e) and homozygous (c, d, and f) neonates (P1) were fixed, embedded in paraffin, sectioned, and stained with HE. The frontal section (a and c) and saggital section (b and d) are shown. BAT is indicated by arrows in panels a to d. The arrow in panel f shows impaired muscle development. Sc, scapular bone; B, BAT. (g and h) The expression of Meltrin α mRNA in heterozygous embryos was detected by in situ hybridization. At E14.5, Meltrin α is expressed in bones, muscles, and the peripheral region of condensing interscapular mesenchymal cells. (Panel h shows an enlarged region of panel g [boxed].)

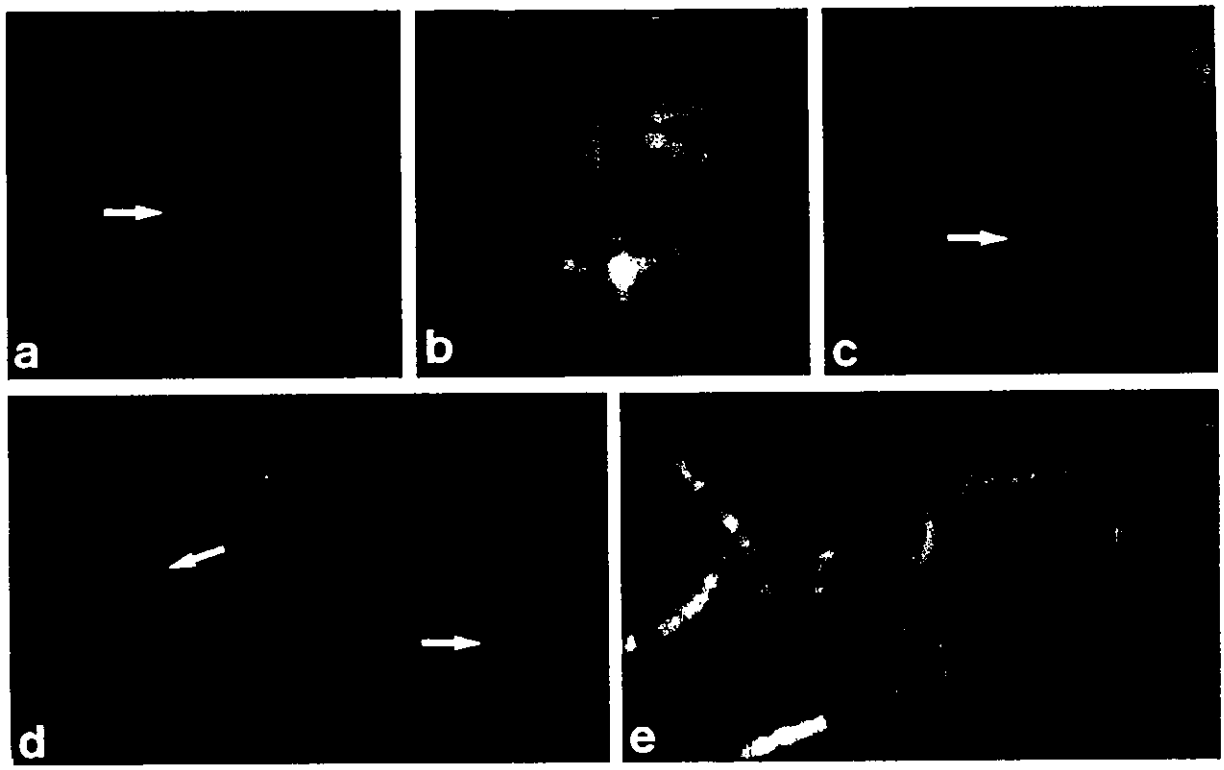

FIG. 4. Chromosomal localization of the Meltrin α gene. Chromosomal localization of the Meltrin α gene on R-banded murine (a to c) and rat (d and e) chromosomes. The chromosomal locations of the murine and rat Meltrin α genes were determined by using a murine cDNA fragment as a biotinylated probe. The hybridization signals are indicated by arrows. The signals are localized to murine chromosome 7F3 distal −F4 and to the rat chromosome 1q43 (proximal). The metaphase spreads were photographed with Nikon B-2A (a, c, and d) and UV-2A (b and e) filters. R-band and G-band patterns are demonstrated in panels a, c, and d and in panels b and e, respectively.

demonstrated that transgenic mice overexpressing Meltrin α have an upregulated formation of adipose tissues (16). Together, these results suggest that Meltrin-α plays regulatory roles in the formation of muscle and adipose tissues.

Recently, experiments with metalloprotease inhibitors have also implicated Meltrin α in cardiac hypertrophy and in the ectodomain shedding of HB-EGF (1). Although the hearts of the Meltrin $\alpha^{-/-}$ mice appear normal, it will be of interest to test whether hypertrophy occurs under conditions of pressure overload. However, we did find that Meltrin α indeed contributes to TPA-stimulated HB-EGF ectodomain shedding in embryonic fibroblasts. The importance of HB-EGF in adipogenesis has not been examined, although its expression in interscapular mesenchymal cells has been observed (unpublished data). On the other hand, insulin-like growth factor I (IGF-I) (32) is one of the cytokines that plays an essential role in adipogenesis and stimulates myogenesis (11, 24, 25). Meltrin α interacts with IGFBP-3 and cleaves it in vitro (19, 36), suggesting that Meltrin α may also regulate the release of active IGFs in BAT and muscle cell lineages by cleaving IGFBPs.

It is not clear at this stage why the levels of penetrance of neonatal lethality, BAT malformation, and hypotrophic muscle formation are so low in the Meltrin α-null mutants. It is possible that other ADAMs may compensate for the loss of Meltrin α due to functional redundancy between Meltrin α and other ADAMs.

ACKNOWLEDGMENTS

This work was supported in part by a grant-in-aid for Scientific Research on Priority Areas from the Ministry of Education, Culture, Sports, Science, and Technology and by research grants from the Japanese Health Science Foundation, the National Center of Neurology and Psychiatry of the Ministry of Health and Welfare of Japan, and CREST (Core Research for Evolutional Science and Technology) of the Japan Science and Technology Corporation.

We thank T. Obata for technical assistance, T. Fujimori for helpful comments, and R. T. Yu for critically reading the manuscript.

REFERENCES

1. **Asakura, M., M. Kitakaze, S. Takashima, Y. Liao, F. Ishikura, T. Yoshinaka, H. Ohmoto, K. Node, K. Yoshino, H. Ishiguro, H. Asanuma, S. Sanada, Y. Matsumura, H. Takeda, S. Beppu, M. Tada, M. Hori, and S. Higashiyama.** 2002. Cardiac hypertrophy is inhibited by antagonism of ADAM12 processing of HB-EGF: metalloproteinase inhibitors as a new therapy. Nat. Med. 8:35–40.
2. **Black, R. A., C. T. Rauch, C. J. Kozlosky, J. J. Peschon, J. L. Slack, M. F. Wolfson, B. J. Castner, K. L. Stocking, P. Reddy, S. Srinivasan, N. Nelson, N. Boiani, K. A. Schooley, M. Gerhart, R. Davis, J. N. Fitzner, R. S. Johnson, R. J. Paxton, C. J. March, and D. P. Cerretti.** 1997. A metalloproteinase disintegrin that releases tumour-necrosis factor-alpha from cells. Nature 385:729–733.
3. **Black, R. A., and J. M. White.** 1998. ADAMs: focus on the protease domain. Curr. Opin. Cell Biol. 10:654–659.
4. **Blobel, C. P., T. G. Wolfsberg, C. W. Turck, D. G. Myles, P. Primakoff, and J. M. White.** 1992. A potential fusion peptide and an integrin ligand domain in a protein active in sperm-egg fusion. Nature 356:248–252.
5. **Borneman, A., R. Kuschel, and A. Fujisawa-Sehara.** 2000. Analysis for transcript expression of meltrin alpha in normal, regenerating, and denervated rat muscle. J. Muscle Res. Cell Motil. 21:475–480.
6. **Bridges, L. C., P. H. Tani, K. R. Hanson, C. M. Roberts, M. B. Judkins, and**

R. D. Bowditch. 2002. The lymphocyte metalloprotease MDC-L (ADAM 28) is a ligand for the integrin $\alpha_4\beta_1$. J. Biol. Chem. 277:3784–3792.
7. Buxbaum, J. D., K. N. Liu, Y. Luo, J. L. Slack, K. L. Stocking, J. J. Peschon, R. S. Johnson, B. J. Castner, D. P. Cerretti, and R. A. Black. 1998. Evidence that tumor necrosis factor alpha converting enzyme is involved in regulated alpha-secretase cleavage of the Alzheimer amyloid protein precursor. J. Biol. Chem. 273:27765–27767.
8. Cho, C., D. O. Bunch, J. E. Faure, E. H. Goulding, E. M. Eddy, P. Primakoff, and D. G. Myles. 1998. Fertilization defects in sperm from mice lacking Fertilin β. Science 281:1857–1859.
9. Dangain, J., and G. Vrbova. 1984. Muscle development in *mdx* mutant mice. Muscle Nerve 7:700–704.
10. Eto, K., W. Puzon-McLaughlin, D. Sheppard, A. Sehara-Fujisawa, X. P. Zhang, and Y. Takada. 2000. RGD-independent binding of integrin alpha9beta1 to the ADAM-12 and -15 disintegrin domains mediates cell-cell interaction. J. Biol. Chem. 275:34922–34930.
11. Florini, J. R., D. Z. Ewton, and S. A. Coolican. 1996. Growth hormone and the insulin-like growth factor system in myogenesis. Endocrinol. Rev. 17: 481–517.
12. Gilpin, B. J., F. Loechel, M. G. Mattei, E. Engvall, R. Albrechtsen, and U. M. Wewer. 1998. A novel, secreted form of human ADAM 12 (Meltrin α) provokes myogenesis in vivo. J. Biol. Chem. 273:157–166.
13. Goishi, K., S. Higashiyama, M. Klagsbrun, M. Ishikawa, E. Mekada, and N. Taniguchi. 1995. Phorbol ester induces the rapid processing of cell surface heparin-binding EGF-like growth factor: conversion from juxtacrine to paracrine growth factor activity. Mol. Biol. Cell 6:967–980.
14. Hogan, B., R. Beddington, F. Costantini, and E. Lacy. 1994. Manipulating the mouse embryo: a laboratory manual. Cold Spring Harbor Laboratory Press, Cold Spring Harbor, N.Y.
15. Iba, K., R. Albrechtsen, B. Gilpin, C. Frohlich, F. Loechel, A. Zolkiewska, K. Ishiguro, T. Kojima, W. Liu, J. K. Langford, R. D. Sanderson, C. Brakebusch, R. Fassler, and U. M. Wewer. 2000. The cysteine-rich domain of human ADAM 12 supports cell adhesion through syndecans and triggers signaling events that lead to beta1 integrin-dependent cell spreading. J. Cell Biol. 149:1143–1156.
16. Kawaguchi, N., X. Xu, R. tajima, P. Kronqvist, C. Sundberg, F. Loechel, R. Albrechtsen, and U. M. Wewer. 2002. ADAM 12 protease induces adipogenesis in transgenic mice. Am. J. Pathol. 160:1895–1903.
17. Kurisaki, T., A. Masuda, N. Osumi, Y. Nabeshima, and A. Fujisawa-Sehara. 1998. Spatially- and temporally-restricted expression of meltrin α (ADAM12) and β (ADAM19) in mouse embryo. Mech. Dev. 73:211–215.
18. Lieber, T., S. Kidd, and M. W. Young. 2002. Kuzbanian-mediated cleavage of *Drosophila* Notch. Genes Dev. 16:209–221.
19. Loechel, F., J. W. Fox, G. Murphy, R. Albrechtsen, and U. M. Wewer. 2000. ADAM 12-S cleaves IGFBP-3 and IGFBP-5 and is inhibited by TIMP-3. Biochem. Biophys. Res. Commun. 278:511–515.
20. Lyon, M. F., Y. Cocking, and X. Gao. 1996. Mouse chromosome atlas. Mouse Genome 95:731–798.
21. Matsuda, Y., Y. N. Harada, S. Natsuume-Sakai, K. Lee, T. Shiomi, and V. M. Chapman. 1992. Location of the mouse complement factor H gene (cfh) by FISH analysis and replication R-banding. Cytogenet. Cell Genet. 61:282–285.
22. Matsuda, Y., T. Imai, T. Shiomi, T. Saito, M. Yamauchi, T. Fukao, Y. Akao, N. Seki, H. Ito, and T. A. Hori. 1996. Comparative genome mapping of the ataxia-telangiectasia region in mouse, rat, and Syrian hamster. Genomics 34:347–352.
23. Moss, M. L., S. L. Jin, M. E. Milla, D. M. Bickett, W. Burkhart, H. L. Carter, W. J. Chen, W. C. Clay, J. R. Didsbury, D. Hassler, C. R. Hoffman, T. A. Kost, M. H. Lambert, M. A. Leesnitzer, P. McCauley, G. McGeehan, J. Mitchell, M. Moyer, G. Pahel, W. Rocque, L. K. Overton, F. Schoenen, T. Seaton, J. L. Su, J. D. Becherer, et al. 1997. Cloning of a disintegrin metalloproteinase that processes precursor tumour necrosis factor-alpha. Nature 385:733–736.
24. Musaro, A., K. McCullagh, A. Paul, L. Houghton, G. Dobrowolny, M. Molinaro, E. R. Barton, H. L. Sweeney, and N. Rosenthal. 2001. Localized Igf-1 transgene expression sustains hypertrophy and regeneration in senescent skeletal muscle. Nat. Genet. 27:195–200.
25. Musaro, A., K. J. McCullagh, F. J. Naya, E. N. Olson, and N. Rosenthal. 1999. IGF-1 induces skeletal myocyte hypertrophy through calcineurin in association with GATA-2 and NF-ATc1. Nature 400:581–585.
26. Nagy, A., J. Rossant, R. Nagy, W. Abramow-Newerly, and J. C. Roder. 1993. Derivation of completely cell culture-derived mice from early-passage embryonic stem cells. Proc. Natl. Acad. Sci. USA 90:8424–8428.
27. Nath, D., P. M. Slocombe, A. Webster, P. E. Stephens, A. J. Docherty, and G. Murphy. 2000. Meltrin γ (ADAM-9) mediates cellular adhesion through $\alpha_6\beta_1$ integrin, leading to a marked induction of fibroblast cell motility. J. Cell Sci. 113(Pt. 12):2319–2328.
28. Pan, D., and G. M. Rubin. 1997. Kuzbanian controls proteolytic processing of Notch and mediates lateral inhibition during *Drosophila* and vertebrate neurogenesis. Cell 90:271–280.
29. Pittenger, M. F., A. M. Mackay, S. C. Beck, R. K. Jaiswal, R. Douglas, J. D. Mosca, M. A. Moorman, D. W. Simonetti, S. Craig, and D. R. Marshak. 1999. Multilineage potential of adult human mesenchymal stem cells. Science 284:143–147.
30. Primakoff, P., and D. G. Myles. 2000. The ADAM gene family: surface proteins with adhesion and protease activity. Trends Genet. 16:83–87.
31. Qi, H., M. D. Rand, X. Wu, N. Sestan, W. Wang, P. Rakic, T. Xu, and S. Artavanis-Tsakonas. 1999. Processing of the Notch ligand delta by the metalloprotease Kuzbanian. Science 283:91–94.
32. Rosen, E. D., and B. M. Spiegelman. 2000. Molecular regulation of adipogenesis. Annu. Rev. Cell Dev. Biol. 16:145–171.
33. Sambrook, J., E. F. Fritsch, and T. Maniatis. 1989. Molecular cloning: a laboratory manual. Cold Spring Harbor Laboratory Press, Cold Spring Harbor, N.Y.
34. Satoh, H., M. C. Yoshida, and M. Sasaki. 1989. High resolution chromosome banding in the Norway rat, *Rattus norvegicus*. Cytogenet. Cell Genet. 50:151–154.
35. Schlondorff, J., and C. P. Blobel. 1999. Metalloprotease-disintegrins: modular proteins capable of promoting cell-cell interactions and triggering signals by protein-ectodomain shedding. J. Cell Sci. 112(Pt. 21):3603–3617.
36. Shi, Z., W. Xu, F. Loechel, U. M. Wewer, and L. J. Murphy. 2000. ADAM 12, a disintegrin metalloprotease, interacts with insulin-like growth factor-binding protein-3. J. Biol. Chem. 275:18574–18580.
37. Shirakabe, K., S. Wakatsuki, T. Kurisaki, and A. Fujisawa-Sehara. 2001. Roles of Meltrin β/ADAM19 in the processing of neuregulin. J. Biol. Chem. 276:9352–9358.
38. Somssich, I. E., and H. Hameister. 1996. Standard karyotype of early replicating bands (RBG-banding), p. 1450–1451. *In* M. F. Lyon, S. Rastan, and S. D. M. Brown (ed.), Genetic variants and strains of the laboratory mouse. Oxford University Press, Oxford, England.
39. Soriano, P., C. Montgomery, R. Geske, and A. Bradley. 1991. Targeted disruption of the c-*src* proto-oncogene leads to osteopetrosis in mice. Cell 64:693–702.
40. Sotillos, S., F. Roch, and S. Campuzano. 1997. The metalloprotease-disintegrin Kuzbanian participates in Notch activation during growth and patterning of *Drosophila* imaginal discs. Development 124:4769–4779.
41. Stedman, H. H., H. L. Sweeney, J. B. Shrager, H. C. Maguire, R. A. Panettieri, B. Petrof, M. Narusawa, J. M. Leferovich, J. T. Sladky, and A. M. Kelly. 1991. The *mdx* mouse diaphragm reproduces the degenerative changes of Duchenne muscular dystrophy. Nature 352:536–539.
42. Taylor, S. M., and P. A. Jones. 1979. Multiple new phenotypes induced in 10T1/2 and 3T3 cells treated with 5-azacytidine. Cell 17:771–779.
43. Turner, A. J., and N. M. Hooper. 1999. Role for ADAM-family proteinases as membrane protein secretases. Biochem. Soc. Trans. 27:255–259.
44. Wolfsberg, T. G., P. Primakoff, D. G. Myles, and J. M. White. 1995. ADAM, a novel family of membrane proteins containing a disintegrin and metalloprotease domain: multipotential functions in cell-cell and cell-matrix interactions. J. Cell Biol. 131:275–278.
45. Yagami-Hiromasa, T., T. Sato, T. Kurisaki, K. Kamijo, Y. Nabeshima, and A. Fujisawa-Sehara. 1995. A metalloprotease-disintegrin participating in myoblast fusion. Nature 377:652–656.
46. Yagi, T., S. Nada, N. Watanabe, H. Tamemoto, N. Kohmura, Y. Ikawa, and S. Aizawa. 1993. A novel negative selection for homologous recombinants using diphtheria toxin A fragment gene. Anal. Biochem. 214:77–86.
47. Yamada, J., T. Kuramoto, and T. Serikawa. 1994. A rat genetic linkage map and comparative maps for mouse or human homologous rat genes. Mamm. Genome 5:63–83.
48. Zhou, M., R. Graham, G. Russell, and P. I. Croucher. 2001. MDC-9 (ADAM-9/Meltrin γ) functions as an adhesion molecule by binding the $\alpha_v\beta_5$ integrin. Biochem. Biophys. Res. Commun. 280:574–580.